EMEP Report 1/2020
Date: May 15, 2020

METEOROLOGISK INSTITUTT
Norwegian Meteorological Institute

Transboundary particulate matter, photo-oxidants, acidifying and eutrophying components

EMEP/MSC-W:	Hilde Fagerli, Svetlana Tsyro, Jan Eiof Jonson, Ágnes Nyíri, Michael Gauss, David Simpson, Peter Wind, Anna Benedictow, Heiko Klein, Augustin Mortier
EMEP/CCC:	Wenche Aas, Anne-Gunn Hjellbrekke, Sverre Solberg, Stephen Matthew Platt, Karl Espen Yttri, Kjetil Tørseth
EMEP/CEIP:	Silke Gaisbauer, Katarina Mareckova, Bradley Matthews, Sabine Schindlbacher, Carlos Sosa, Melanie Tista, Bernhard Ullrich, Robert Wankmüller
CCE/UBA:	Thomas Scheuschner
Chalmers Univ. Tech.	Robert Bergström (on leave from SMHI)
FMI:	Lasse Johanson, Jukka-Pekka Jalkanen
ResearchConcepts:	Swen Metzger
TNO:	Hugo A.C. Denier van der Gon, Jeroen J.P. Kuenen, Antoon J.H. Visschedijk
Univ. of Gothenburg:	Lars Barregård, Peter Molnár, Leo Stockfelt

EMEP Status Report 2020; May 15, 2020

ISSN 1504-6109 (print)
ISSN 1504-6192 (on-line)

OLD-OLD-OLD Executive Summary

This report presents the EMEP activities in 2018 and 2019 in relation to transboundary fluxes of particulate matter, photo-oxidants, acidifying and eutrophying components, with focus on results for 2017. It presents major results of the activities related to emission inventories, observations and modelling. The report also introduces specific relevant research activities addressing EMEP key challenges, as well as technical developments of the observation and modelling capacities.

Measurements and model results for 2017

In the first chapter, the status of air pollution in 2017 is presented, combining meteorological information and emissions with numerical simulations using the EMEP MSC-W model together with observed air concentration and deposition data.

Altogether 35 Parties reported measurement data for 2017, from 171 sites in total. Of these, 139 sites reported measurements of inorganic ions in precipitation and/or main components in air; 75 of these sites had co-located measurements in both air and precipitation. The ozone network consisted of 139 sites, particulate matter was measured at 69 sites, of which 50 performed measurements of both PM_{10} and $PM_{2.5}$. In addition, 45 sites reported at least one of the components required in the advanced EMEP measurement program (level 2). A complete aerosol program was implemented at 8 sites, while only a few sites provided the required oxidant precursor measurements.

The mean daily max O_3, SOMO35 and AOT40 all show a distinct gradient with levels increasing from north to south, a well established feature for ozone reflecting the dependency of ozone on the photochemical conditions. The geographical pattern in the measured values is fairly well reflected by the model results for all these three metrics. In particular, the modelled mean daily max for the summer half year agrees very well with the measured values except for an underestimation in a few regions, mainly in the Mediterranean. Particularly high levels are predicted by the model in the south-east, but due to the lack of monitoring sites these levels could not be validated.

The model results and the observations agree quite well on the geographical distribution of annual mean PM_{10} and $PM_{2.5}$, with concentrations below 2-5 μg m^{-3} in northern Europe, increasing to 5-15 μg m^{-3} in central Europe and further south. The regional background PM is fairly homogeneous over most of central and western Europe, with somewhat elevated PM_{10} and $PM_{2.5}$ levels of 15-20 μg m^{-3} modelled for the Po Valley, the Benelux countries, and also

observed in Poland, Czechia, Hungary and Spain. On average, the model underestimates the observed 2017 annual mean PM_{10} and $PM_{2.5}$ by 22% and 19% with annual mean spatial correlation coefficients of 0.76 and 0.81, respectively.

Due to meteorological conditions, the annual mean PM_{10} and $PM_{2.5}$ concentrations were 5 to 20% lower in 2017 compared to the 5-year (2012-2016) mean over central, eastern and south-eastern Europe, and the North Atlantic coast, with the largest negative anomalies of 20-30% seen over northern and north-western Europe. Due to the combined effect of meteorology and emission changes, annual mean PM_{10} and $PM_{2.5}$ in 2017 were considerably lower compared to the average levels in the 2000s, by 5-20% over Spain, Portugal and Italy and most of Russia, and by as much as 20-35% in many parts of northern, western and central Europe. In addition to emission reductions, 2017 was a meterologically favorable year in terms of air pollution removal by precipitation.

Exceedances and pollution episodes in 2017

In 2017, relatively few high ozone episodes were experienced in central and northern Europe whereas southern Europe, in particular the Po Valley and the Iberian Peninsula, experienced a number of episodes of smaller regional extent. An intense heat wave (named Lucifer) struck parts of southern Europe (south-east France, Italy, the Balkans) in early August, described as the worst heat wave since 2003 here. The highest ozone level observed, 119.5 ppb (239 μg m^{-3}), was just below EUs alert level of 240 μg m^{-3}, and was recorded at the rural background site Parco La Mandria in north-west Italy (data from the EEA data base). The EMEP MSC-W model reproduce the observed geographical extent of the episode very well, but underpredicts the peak values in many areas.

Model results and EMEP observational data show that in 2017, the annual mean PM_{10} and $PM_{2.5}$ concentrations were below the EU limit values for all of Europe. However, exceedences of the Air Quality Guideline (AQG) recommended by WHO (10 μg m^{-3}) in the annual mean of $PM_{2.5}$ were observed at ten sites.

Exceedance days for PM_{10} were observed at 35 out of 58 sites, but no violations of the PM_{10} EU limit value (more than 35 exceedance days) were registered. 18 sites had more than 3 exceedance days, the recommended AQG by WHO. $PM_{2.5}$ concentrations exceeded the WHO AQG value at 35 out of 46 stations in 2017 (on more than 3 days at 26 sites).

The largest PM pollution episodes occurred in January-February and affected air quality in many European countries. The timeseries of modelled and observed chemical composition of $PM_{2.5}$ at selected sites in France, Poland and Czechia (and also modelled PM_{10} chemical composition for several sites in central and eastern Europe), during the January-February 2017 episodes indicate a diversity of emission sources causing the episodes at different locations.

Critical loads (CL) for eutrophication were exceeded in virtually all countries in 2017, in about 63.9% of the ecosystem area, and the European average exceedance was about 277 eq ha^{-1}yr^{-1}. The highest exceedances are found in the Po Valley in Italy, the Dutch-German-Danish border areas and in north-east Spain. In contrast, critical loads of acidity were not exceeded in most of Europe. Hot spots of exceedances can be found in the Netherlands and its border areas to Germany and Belgium, and some smaller maximum in southern Germany and the Czechia. In Europe as a whole, acidity exceedances in 2017 occur in about 5.5% of the ecosystem area, and the European average exceedance is about 32.4 eq ha^{-1}yr^{-1}.

Status of emissions

In 2019, 45 out of 51 Parties (88%) submitted emission inventories to the EMEP Centre on Emission Inventories and Projections (CEIP). The quality of reported data differs significantly across countries, and the uncertainty of the data is considered to be relatively high.

Under the auspices of the *EU Action on Black Carbon in the Arctic* a technical report was recently compiled. The report reviewed, inter alia, the level of BC reporting under the LRTAP Convention. Despite a large number of Parties voluntarily reporting BC emissions, the review revealed a number of shortcomings. As of 2018, nine Parties had not yet submitted BC emissions inventories to the Convention. Furthermore, significant issues in terms of consistency, completeness and comparability were found in the reported emissions. For the majority of the Parties which reported emissions for 2017, BC emissions constitute between 10 and 20% of the respective total $PM_{2.5}$ emissions.

The condensable component of particulate matter is probably the largest single source of uncertainty in PM emissions. Currently the condensable component is not included or excluded consistently in PM emissions reported by Parties of the LRTAP Convention. Parties were asked to include a table with information on the inclusion of the condensable component in PM_{10} and $PM_{2.5}$ emission factors for the reporting under the CLRTAP convention in 2019. This table was added to the revised recommended structure for informative inventory reports. This year, 17 Parties provided information on the inclusion of the condensable component. However, the reporting in 2019 showed that in many cases Parties do not have information on whether or not the PM emissions of a specific source category include the condensable component. The status of inclusion or exclusion is best known for the emissions from road transport, whilst it is less clear for small-scale combustion sources.

2017 was the first year with reporting obligation of gridded emissions in $0.1^\circ \times 0.1^\circ$ longitude/latitude resolution. Until June 2019, thirty of the 48 countries which are considered to be part of the EMEP area reported sectoral gridded emissions in this resolution. For remaining areas missing emissions are gap-filled and spatially distributed using expert estimates. This year CEIP also performed gap-filling and gridding for the whole time series from 1990 to 2017 in $0.1^\circ \times 0.1^\circ$ longitude/latitude resolution on GNFR sector level for the main pollutants, and from 2000 to 2017 for PMs. Emissions from international shipping in different European seas were updated based on the CAMS global shipping emission dataset for the years 2000 to 2017, provided via ECCAD *CAMS_GLOB_SHIP*. Shipping emissions from 1990 to 1999 were estimated using CAMS global shipping emissions for 2000, adjusted with trends for global shipping from EDGAR v.4.3.2.

The 1999 Gothenburg Protocol lists emission reduction commitments of NO_x , SO_x, NH_3 and NMVOCs for most of the Parties to the LRTAP Convention for the year 2010. These commitments should not be exceeded in 2010 nor in subsequent years. When considering only reported data, approved adjustments and fuel use data of the respective countries, it can be seen that the Netherlands and USA had not reduce their NMVOC emissions according to the Gothenburg Protocol requirements, and that Croatia, Germany, Norway and Spain are above their Gothenburg Protocol ceilings for NH_3. In terms of NO_x emissions, Norway exceeded its ceilings.

Condensable organics; issues and implications for EMEP calculations and source-receptor matrices

Estimates of PM and NMVOC emissions as currently provided by Parties have a number of major uncertainties, and there is a clear need for clarification and standardisation of the meth-

ods used to define and report PM emissions, also concerning the fraction of PM that is primary organic aerosol (POA). For example, emissions from residential wood-burning in Europe represent around 50% of Europe's POA emissions, and they dominate wintertime POA sources, but several studies show that the definitions behind national emission estimates are inconsistent in their treatment of condensable organic compounds. A new bottom-up emissions inventory for OA was implemented for this study, taking account of condensable organics. For some countries (e.g. NO, DK) the bottom-up and EMEP estimates of $PM_{2.5}$ emissions are comparable, but for others (e.g. FI, SE) the expert estimates are far higher than the reported emissions. The new inventory gave improved model performance for organic aerosol and thus $PM_{2.5}$, especially in wintertime. We show that source-receptor calculations are also sensitive to these uncertainties, both for $PM_{2.5}$ and especially for organic aerosol contributions. Such inconsistencies pose grave problems for the modeling of $PM_{2.5}$ and for any analysis of emission control strategies or cost-benefit analysis. In the worst case these problems might lead to wrong priorities of measures. A review and harmonisation of methods for PM and POA emission inventories is recommended.

The EMEP Intensive Measurement Period (EIMP) 2017/18: Equivalent Black Carbon (EBC) from fossil fuel and biomass burning sources

In this report we present results from the ongoing analysis of data from the EMEP IMP 2017/18. We present source apportionment of equivalent black carbon into fossil and biomass fractions (EBC_{ff} and EBC_{bb}, respectively), using the aethalometer model and positive matrix factorization (PMF). According to the aethalometer model, EBC_{bb} represents between close to zero (e.g. Beirut, Lebanon) and just over 50 % (e.g. Beograd, Serbia) of background EBC. However, this model requires a priori knowledge of the aerosol Ångström exponent (AAE), and results from the aethalometer model vary widely depending on the input AAEs. Using a new application of PMF to aethalometer data, we were able to identify EBC_{ff} and EBC_{bb} results without input AAEs (rather AAEs are an output derived from factor profiles).

EMEP MSC-W model calculations were performed for the time period of the EMEP EIMP, using several sources of EC emission data, including the reported EMEP EC emissions. The resulting modelled EC concentrations and the share of EC concentrations from biomass burning (EC_{bb}) and fossil fuel (EC_{ff}) sources were compared to the preliminary data available from the EIMP (EBC and biomass burning fractions from PMF). The results suggest that the EC emissions are somewhat low (or the spatial distributions are erroneous) for this winter period, especially in the reported EMEP EC emission inventory. All the model results show reasonable agreement with observations at rural sites, whilst there is no correlation between model results and observations at urban sites (and even anti-correlation when reported EMEP EC emissions are used).

The fractions of EC emissions from biomass burning sources versus fossil fuel are very different in the reported EMEP emissions and in the emission data set developed by TNO (CAMS_2015_RWC), resulting in substantially different modelled EC_{bb}/EC_{ff} concentration fractions. Model calculations based on reported EMEP EC emissions are in reasonable agreement with the PMF values for biomass burning fractions, whilst model results based on CAMS_2015_RWC give consistently higher biomass burning fractions than PMF. Given that the reported EC emissions might be somewhat low, the proportion of different EC sources in the EMEP emission data could be approximately correct for the wrong reasons, as the emissions from different sources (with completely independent emission factors) would have to increase proportionally to keep the biomass burning fraction about the same.

Only a subset of the EIMP data has been used in this analyses, and measurement data will become available for more sites in the near future. Further investigations, including in depth analyses of model results at the different rural and urban EIMP sites and spatial distribution of emissions for different emission sectors, are needed to determine the validity and possible implications of these preliminary results.

The EMEP trend interface

A new trend interface is under development at MSC-W (available at `http://aerocom.met.no/trends/EMEP/`). The trend interface is designed for visualization of the long-term modelling results at all EMEP sites that have reported observations to EMEP/CCC. A range of new functionalities have been implemented in the interface since last year, the most important being inclusion of EMEP observations and model evaluation statistics. The interface has been extended to include more species, and now visualizes data for ozone, PM_{10} and $PM_{2.5}$. Furthermore, the impacts from different emission sectors on PM_{10} and $PM_{2.5}$ concentrations are vizualised and a number of other technical facilities have been introduced.

Evaluation of the gridded EMEP 0.1°×0.1° emissions using modelling

EMEP MSC-W model results using the EMEP $0.1°\times0.1°$ resolution emissions have been compared to model results using the older 50km × 50km resolution and to model results using CAMS-REG-AP - a widely used set of fine resolution emissions ($0.1° \times 0.05°$) developed by TNO. The three sets of model results have been compared to AirBase observations for each country individually, focusing on the spatial distribution of the results. The largest improvement in going from 50km × 50km resolution to $0.1°\times0.1°$ resolution is seen for NO_2, which can be explained by the high correlations between emissions and surface concentrations of NO_2. Interestingly, for NO_2 the model results using the EMEP $0.1°\times0.1°$ resolution emissions have higher (or similar) spatial correlation compared to observations for most countries than model results based on CAMS-REG-AP, suggesting that the gridding performed by the countries are superior to the gridding done for CAMS-REG-AP. This may not be surprising, as the gridding done by the countries in most cases are based on national data, that are probably better than the European-wide proxies used for CAMS-REG-AP. For some countries, the model runs with fine resolution EMEP emissions showed substantially worse correlation to observations than the CAMS-REG-AP fine resolution emissions. For these countries it would be worthwhile looking further into the methodology used for spatial distribution of the emissions.

Baltic Sea shipping

As part of the EU Interreg project EnviSum the effects of emissions from Baltic Sea shipping on air pollution and health have been calculated, and the results published in two journal papers. A resume of the papers is given in this report. We find that the implementation of the stricter SECA regulations from January 2015 has been successful in reducing sulphur emissions from shipping. As a result, $\mathrm{PM_{2.5}}$ concentrations, in particular in coastal zones, have been reduced. A large portion of the population in the Baltic Sea region lives in the coastal zones. The stricter SECA regulations have alleviated the health burden in the region by reducing the mortality and morbidity from Baltic Sea shipping by about one third. The main source of $\mathrm{PM_{2.5}}$ from the Emission Control Areas in the Baltic Sea (and the North Sea) is now $\mathrm{NO_x}$, and the resulting health effects are still significant. $\mathrm{NO_x}$ will be regulated from 2021 in the region, but only for new ships, resulting in only a gradual decrease in emissions.

Model improvements

The model version used for reporting this year has some significant changes since the rv4.17a documented last year. A new gas-phase chemical mechanism has been introduced (EmChem19), which is a substantial revision of the EmChem16 scheme used previously. The reaction rates in EmChem19 are updated to be consistent with the latest recommendations from the IUPAC. In addition to these updates some new gas-phase reactions have been added and a few new chemical species have been included in the chemical mechanism, in order to be more consistent with the Master Chemical Mechanism (MCM). An error in the calculations of photosynthetically active radiation (PAR) has been fixed, impacting mainly the ozone uptake for forests.

The latest version of the Equlibrium Simplified Aerosol Model V4 (EQSAM4clim), has been implemented in the EMEP MSC-W model as one of the alternative schemes to calculate gas/aerosol partitioning. First tests show that the results from EQSAM4clim are very similar, or slightly better, than those obtained with the MARS thermodynamic scheme. The advantage of EQSAM4clim is that the scheme allows completing the thermodynamic equilibrium with missing cations and anions from sea salt and mineral dust, which is anticipated to further improve EQSAM4clim performance.

In addition, a number of technical improvements with respect to flexibility and usability of the model have been made.

Development in the monitoring network and database infrastructure

The last chapter of the report presents the implementation of the EMEP monitoring strategy and general development in the monitoring programme including data submission. There are large differences between Parties in the level of implementation, as well as significant changes in the national activities during the period 2000-2017. With respect to the requirement for level 1 monitoring, 40% of the Parties have had an improvement since 2010, while 33% have reduced the level of monitoring. For level 2 monitoring there has been a general positive development in recent years. However, only few sites have a complete measurement program.

The complexity of data reporting has increased in recent years, and it is therefore now mandatory for the data providers to use the submission and validation tool when submitting data to EMEP to improve the quality and timeliness in the data flow. There is a need for improvements in the reporting, as only half of the data providers use the submission tool, and less than 60% report within the deadline of 31 July.

OLD-OLD-OLD Acknowledgments

This work has been funded by the EMEP Trust Fund.

The development of the EMEP MSC-W model has also been supported by Copernicus Atmosphere Modelling Service (CAMS) projects, the Nordic Council of Ministers, the Norwegian Space Centre and the Norwegian Ministry of Climate and Environment. Development work has also been supported at Chalmers University of Technology in Sweden using funds from the Swedish Strategic Research project MERGE, the framework research program on 'Photochemical smog in China' financed by the Swedish Research Council (639-2013-6917), and FORMAS.

The work on condensable organics was partly funded by the Norwegian Ministry of Climate and Environment. The work of TNO was funded to a large extent by the Copernicus Atmosphere Monitoring Service (CAMS), in particular the Contracts on emissions (CAMS_81) and policy products (CAMS_71).

The work presented in this report has benefited largely from the work carried out under the four EMEP Task Forces and in particular under TFMM.

A large number of co-workers in participating countries have contributed in submitting quality assured data. The EMEP centers would like to express their gratitude for continued good co-operation and effort. The institutes and persons providing data are listed in the EMEP/CCC's data report and identified together with the data sets in the EBAS database.

For developing standardized methods, harmonization of measurements and improving the reporting guidelines and tools, the close co-operations with participants in the European Research Infrastructure for the observation of Aerosol, Clouds, and Trace gases (ACTRIS) as well as with the Scientific Advisory Groups (SAGs) in WMO/GAW are especially appreciated.

The Working Group on Effects and its ICPs and Task Forces are acknowledged for their assistance in determining the risk of damage from air pollution.

The computations were partly performed on resources provided by UNINETT Sigma2 - the National Infrastructure for High Performance Computing and Data Storage in Norway (grant NN2890k and NS9005k). IT infrastructure in general was available through the Norwegian Meteorological Institute (MET Norway). Furthermore, the CPU time granted on the

supercomputers owned by MET Norway has been of crucial importance for this year's source-receptor matrices and trend calculations. The CPU time made available by ECMWF to generate meteorology has been important for both the source-receptor and status calculations in this year's report.

Contents

CHAPTER 1

OLD-OLD-OLD Introduction

1.1 Purpose and structure of this report

The mandate of the European Monitoring and Evaluation Programme (EMEP) is to provide sound scientific support to the Convention on Long-range Transboundary Air Pollution (LRTAP), particularly in the areas of atmospheric monitoring and modelling, emission inventories, emission projections and integrated assessment. Each year EMEP provides information on transboundary pollution fluxes inside the EMEP area, relying on information on emission sources and monitoring results provided by the Parties to the LRTAP Convention.

The purpose of the annual EMEP status reports is to provide an overview of the status of transboundary air pollution in Europe, tracing progress towards existing emission control Protocols and supporting the design of new protocols, when necessary. An additional purpose of these reports is to identify problem areas, new aspects and findings that are relevant to the Convention.

The present report is divided into four parts. Part I presents the status of transboundary air pollution with respect to acidification, eutrophication, ground level ozone and particulate matter in Europe in 2017. Part II summarizes research activities of relevance to the EMEP programme, while Part III deals with technical developments going on within the centres.

Appendix **??** in Part IV contains information on the national total emissions of main pollutants and primary particles for 2017, while Appendix **??** shows the emission trends for the period of 2000-2017. Country-to-country source-receptor matrices with calculations of the transboundary contributions to pollution in different countries for 2017 are presented in Appendix **??**.

Appendix **??** describes the country reports which are issued as a supplement to the EMEP status reports.

Appendix **??** introduces the model evaluation report for 2017 (Gauss et al. 2019c) which is available online and contains time series plots of acidifying and eutrophying components (Gauss et al. 2019b), ozone (Gauss et al. 2019a) and particulate matter (Tsyro et al. 2019). These plots are provided for all stations reporting to EMEP (with just a few exclusions due to data-capture or technical problems). This online information is complemented by numerical

fields and other information on the EMEP website. The reader is encouraged to visit the website, `http://www.emep.int`, to access this additional information.

1.2 Definitions, statistics used

For sulphur and nitrogen compounds, the basic units used throughout this report are μg (S or N)/m^3 for air concentrations and mg (S or N)/m^2 for depositions. Emission data, in particular in some of the Appendices, is given in Gg (SO_2) and Gg (NO_2) in order to keep consistency with reported values.

For ozone, the basic units used throughout this report are ppb (1 ppb = 1 part per billion by volume) or ppm (1 ppm = 1000 ppb). At 20°C and 1013 mb pressure, 1 ppb ozone is equivalent to 2.00 μg m^{-3} .

A number of statistics have been used to describe the distribution of ozone within each grid square:

Mean of Daily Max. Ozone - First we evaluate the maximum modelled concentration for each day, then we take either 6-monthly (1 April - 30 September) or annual averages of these values.

SOMO35 - The Sum of Ozone Means Over 35 ppb is the indicator for health impact assessment recommended by WHO. It is defined as the yearly sum of the daily maximum of 8-hour running average over 35 ppb. For each day the maximum of the running 8-hours average for O_3 is selected and the values over 35 ppb are summed over the whole year.

If we let A_8^d denote the maximum 8-hourly average ozone on day d, during a year with N_y days (N_y = 365 or 366), then SOMO35 can be defined as:

$SOMO35 = \sum_{d=1}^{d=N_y} \max\left(A_8^d - 35 \text{ ppb}, 0.0\right)$

where the `max` function evaluates $\max(A-B,0)$ to $A-B$ for $A > B$, or zero if $A \leq B$, ensuring that only A_8^d values exceeding 35 ppb are included. The corresponding unit is ppb.days.

POD$_Y$ - Phyto-toxic ozone dose, is the accumulated stomatal ozone flux over a threshold Y, i.e.:

$$\text{POD}_Y = \int \max(F_{st} - Y, 0)\, dt \tag{1.1}$$

where stomatal flux F_{st}, and threshold, Y, are in nmol m^{-2} s^{-1}. This integral is evaluated over time, from the start of the growing season (SGS), to the end (EGS).

For the generic crop and forest species, the suffix gen can be applied, e.g. POD$_{Y,gen}$ (or $AF_{st}1.6_{gen}$) is used for forests. POD was introduced in 2009 as an easier and more descriptive term for the accumulated ozone flux. The definitions of AFst and POD are identical however, and are discussed further in Mills and Simpson (2010). See also Mills et al. (2011a,b) and Mills et al. (2018).

AOT40 - is the accumulated amount of ozone over the threshold value of 40 ppb, i.e..

$$AOT40 = \int \max(O_3 - 40 \text{ ppb}, 0.0)\, dt$$

where the `max` function ensures that only ozone values exceeding 40 ppb are included. The integral is taken over time, namely the relevant growing season for the vegetation concerned. The corresponding unit are ppb.hours (abbreviated to ppb.h). The usage and definitions of AOT40 have changed over the years though, and also differ between UNECE and the EU. LRTAP (2009) give the latest definitions for UNECE work, and describes carefully how AOT40 values are best estimated for local conditions (using information on real growing seasons for example), and specific types of vegetation. Further, since O_3 concentrations can have strong vertical gradients, it is important to specify the height of the O_3 concentrations used. In previous EMEP work we have made use of modelled O_3 from 1 m or 3 m height, the former being assumed close to the top of the vegetation, and the latter being closer to the height of O_3 observations. In the Mapping Manual (LRTAP 2009) there is an increased emphasis on estimating AOT40 using ozone levels at the top of the vegetation canopy.

Although the EMEP MSC-W model now generates a number of AOT-related outputs, in accordance with the recommendations of LRTAP (2009) we will concentrate in this report on two definitions:

AOT40$^{\mathbf{uc}}_{f}$ - AOT40 calculated for forests using estimates of O_3 at forest-top (uc: upper-canopy). This AOT40 is that defined for forests by LRTAP (2009), but using a default growing season of April-September.

AOT40$^{\mathbf{uc}}_{c}$ - AOT40 calculated for agricultural crops using estimates of O_3 at the top of the crop. This AOT40 is close to that defined for agricultural crops by LRTAP (2009), but using a default growing season of May-July, and a default crop-height of 1 m.

In all cases only daylight hours are included, and for practical reasons we define daylight for the model outputs as the time when the solar zenith angle is equal to or less than 89°. (The proper UNECE definition uses clear-sky global radiation exceeding 50 W m^{-2} to define daylight, whereas the EU AOT definitions use day hours from 08:00-20:00.). In the comparison of modelled and observed AOT40$^{\text{uc}}_{f}$in chapter 2, we have used the EU AOT definitions of day hours from 08:00-20:00.

The AOT40 levels reflect interest in long-term ozone exposure which is considered important for vegetation - critical levels of 3 000 ppb.h have been suggested for agricultural crops and natural vegetation, and 5 000 ppb.h for forests (LRTAP 2009). Note that recent UNECE workshops have recommended that AOT40 concepts are replaced by ozone flux estimates for crops and forests. (See also Mills and Simpson 2010).

This report includes also concentrations of particulate matter (PM). The basic units throughout this report are μg m^{-3} for PM concentrations and the following acronyms are used for different components to PM:

SOA - secondary organic aerosol, defined as the aerosol mass arising from the oxidation products of gas-phase organic species.

SIA - secondary inorganic aerosols, defined as the sum of sulphate (SO_4^{2-}), nitrate (NO_3^-) and ammonium (NH_4^+). In the EMEP MSC-W model SIA is calculated as the sum: SIA= SO_4^{2-} + NO_3^-(fine) + NO_3^-(coarse) + NH_4^+.

SS - sea salt.

MinDust - mineral dust.

PPM - primary particulate matter, originating directly from anthropogenic emissions. One usually distinguishes between fine primary particulate matter, $PPM_{2.5}$, with aerosol diameters below 2.5 μm and coarse primary particulate matter, PPM_{coarse} with aerosol diameters between 2.5 μm and 10 μm.

$PM_{2.5}$ - particulate matter with aerodynamic diameter up to 2.5 μm. In the EMEP MSC-W model $PM_{2.5}$ is calculated as $PM_{2.5}$ = SO_4^{2-} + NO_3^-(fine) + NH_4^+ + SS(fine) + MinDust(fine) + SOA(fine) + $PPM_{2.5}$ + 0.27 NO_3^-(coarse) + PM25water. (PM25water = PM associated water).

PM_{coarse} - coarse particulate matter with aerodynamic diameter between 2.5μm and 10μm. In the EMEP MSC-W model PM_{coarse} is calculated as PM_{coarse} = 0.73 NO_3^-(coarse)+ SS(coarse) + MinDust(coarse) + PPM_{coarse}.

PM_{10} - particulate matter with aerodynamic diameter up to 10 μm. In the EMEP MSC-W model PM_{10} is calculated as PM_{10} = $PM_{2.5}$ + PM_{coarse}.

In addition to bias, correlation and root mean square the statistical parameter, index of agreement, are used to judge the model's agreement with measurements:

IOA - The index of agreement (IOA) is defined as follows (Willmott 1981, 1982):

$$IOA = 1 - \frac{\sum_{i=1}^{N}(m_i - o_i)^2}{\sum_{i=1}^{N}(|m_i - \bar{o}| + |o_i - \bar{o}|)^2} \tag{1.2}$$

where $\bar{o}$ is the average observed value. Similarly to correlation, IOA can be used to assess agreement either spatially or temporally. When IOA is used in a spatial sense, N denotes the number of stations with measurements at one specific point in time, and m_i and o_i are the modelled and observed values at station i. For temporal IOA, N denotes the number of time steps with measurements, while m_i and o_i are the modelled and observed value at time step i. IOA varies between 0 and 1. A value of 1 corresponds to perfect agreement between model and observations, and 0 is the theoretical minimum.

1.3 The EMEP grid

At the 36^{th} session of the EMEP Steering Body the EMEP Centres suggested to increase spatial resolution and projection of reported emissions from 50×50 km polar stereographic grid to 0.1°×0.1° longitude-latitude grid in a geographic coordinate system (WGS84). The EMEP domain shown in Figure 1.1 covers the geographic area between 30°N-82°N latitude

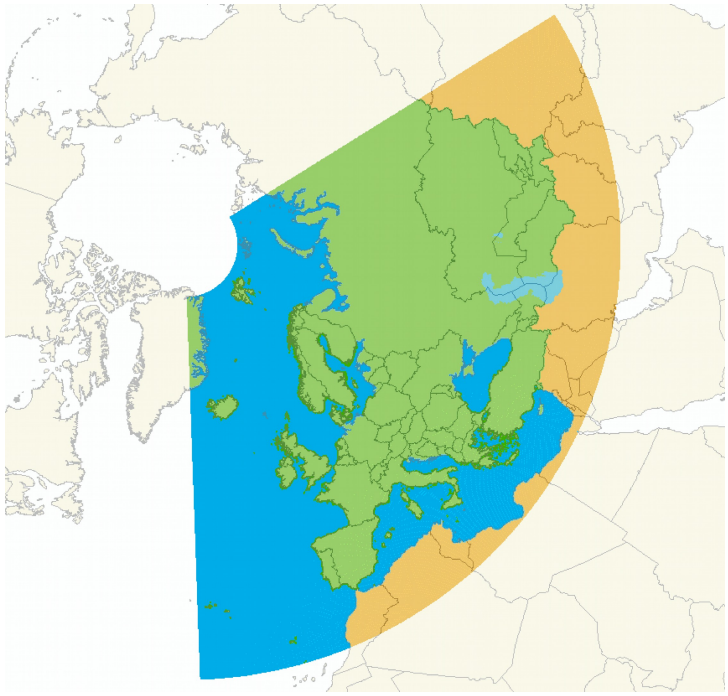

Figure 1.1: The EMEP domain covering the geographic area between 30°N-82°N latitude and 30°W-90°E longitude.

and 30°W-90°E longitude. This domain represents a balance between political needs, scientific needs and technical feasibility. Parties are obliged to report gridded emissions in this grid resolution from year 2017.

The higher resolution means an increase of grid cells from approximately 21500 cells in the 50×50 km^2 grid to 624000 cells in the $0.1°\times0.1°$ longitude-latitude grid.

1.3.1 The reduced grid: EMEP0302

For practical purposes, a coarser grid has also been defined. The EMEP0302 grid covers the same region as the $0.1°\times0.1°$ longitude-latitude EMEP domain (Figure 1.1), but the spatial resolution is 0.3° in the longitude direction and 0.2° in the latitude direction. Each gridcell from the EMEP0302 grid covers exactly 6 gridcells from the $0.1°\times0.1°$ official grid.

1.4 Country codes

Several tables and graphs in this report make use of codes to denote countries and regions in the EMEP area. Table 1.1 provides an overview of these codes and lists the countries and regions included.

All 51 Parties to the LRTAP Convention, except two, are included in the analysis presented in this report. The Parties that are excluded of the analysis are Canada and the United States of America, because they lie outside the EMEP domain.

Code	Country/Region/Source
AL	Albania
AM	Armenia
AST	Asian areas
AT	Austria
ATL	N.-E. Atlantic Ocean
AZ	Azerbaijan
BA	Bosnia and Herzegovina
BAS	Baltic Sea
BE	Belgium
BG	Bulgaria
BIC	Boundary/Initial Conditions
BLS	Black Sea
BY	Belarus
CH	Switzerland
CY	Cyprus
CZ	Czechia
DE	Germany
DK	Denmark
DMS	Dimethyl sulfate (marine)
EE	Estonia
ES	Spain
EU	European Union (EU28)
EXC	EMEP land areas
FI	Finland
FR	France
GB	United Kingdom
GE	Georgia
GL	Greenland
GR	Greece
HR	Croatia
HU	Hungary
IE	Ireland

Code	Country/Region/Source
IS	Iceland
IT	Italy
KG	Kyrgyzstan
KZ	Kazakhstan
LI	Liechtenstein
LT	Lithuania
LU	Luxembourg
LV	Latvia
MC	Monaco
MD	Moldova
ME	Montenegro
MED	Mediterranean Sea
MK	North Macedonia
MT	Malta
NL	Netherlands
NO	Norway
NOA	North Africa
NOS	North Sea
PL	Poland
PT	Portugal
RO	Romania
RS	Serbia
RU	Russian Federation
SE	Sweden
SI	Slovenia
SK	Slovakia
TJ	Tajikistan
TM	Turkmenistan
TR	Turkey
UA	Ukraine
UZ	Uzbekistan
VOL	Volcanic emissions

Table 1.1: Country/region codes used throughout this report.

1.5 Other publications

This report is complemented by a report on EMEP MSC-W model performance for acidifying and eutrophying components, photo-oxidants and particulate matter in 2017 (Gauss et al. 2019c), made available online, at `www.emep.int`.

A list of all associated technical reports and notes by the EMEP centres in 2019 (relevant for transboundary acidification, eutrophication, ozone and particulate matter) follows at the end of this section.

Peer-reviewed publications

The following scientific papers of relevance to transboundary acidification, eutrophication, ground level ozone and particulate matter, involving EMEP/MSC-W and EMEP/CCC staff, have become available in 2018:

Anenberg, S. C., Henze, D. K., Tinney, V., Kinney, P. L., Raich, W., Fann, N., Malley, C. S., Roman, H., Lamsal, L., Duncan, B., Martin, R. V., van Donkelaar, A., Brauer, M., Doherty, R., Jonson, J. E., Davila, Y., Sudo, K., Kuylenstierna, J. C. I. Estimates of the Global Burden of Ambient PM2.5, Ozone, and NO2 on Asthma Incidence and Emergency Room Visits. Environmental Health Perspectives, 126 (10), p. 107004-, 2018. DOI: 10.1289/EHP3766

Bartnicki, J., Semeena, V. S., Mazur, A., Zwozdziak, J. Contribution of Poland to Atmospheric Nitrogen Deposition to the Baltic Sea. Water, Air and Soil Pollution, 229 (353), p. 1-22, 2018. DOI: 10.1007/s11270-018-4009-5

Dong, X., Fu, J. S., Zhu, Q., Sun, J., Tan, J., Keating, T., Sekiya, T., Sudo, K., Emmons, L., Tilmes, S., Jonson, J. E., Schulz, M., Bian, H., Chin, M., Davila, Y., Henze, D., Takemura, T., Benedictow, A. M. K., and Huang, K. Long-range transport impacts on surface aerosol concentrations and the contributions to haze events in China: an HTAP2 multi-model study. Atmos. Chem. Phys., 18, p.15581-15600, 2018. DOI: 10.5194/acp-18-15581-2018

Evangeliou, N., Shevchenko, V. P., Yttri, K. E., Eckhardt, S., Sollum, E., Pokrovsky, O. S., Kobelev, V. O., Korobov, V. B., Lobanov, A. A., Starodymova, D. P., Vorobiev, S. N., Thompson, R. L., and Stohl, A. Origin of elemental carbon in snow from western Siberia and northwestern European Russia during winter-spring 2014, 2015 and 2016. Atmos. Chem. Phys., 18, 963-977, 2018. DOI: 10.5194/acp-18-963-2018

Fleming, Z. L., Doherty, R. M., von Schneidemesser, E., Malley, C. S., Cooper, O. R., Pinto, J. P., Colette, A., Xu, X., Simpson, D., Schultz, M. G., Lefohn, A. S., Hamad, S., Moolla, R., Solberg, S., Feng, Z. Tropospheric Ozone Assessment Report: Present-day ozone distribution and trends relevant to human health. Elementa: Science of the Anthropocene, 6 (12), p. 1-41, 2018. DOI: 10.1525/elementa.273

Galmarini, S., Kioutsioukis, I., Solazzo, E., Alyuz, U., Balzarini, A., Bellasio, R., Benedictow, A. M. K., Bianconi, R., Bieser, J., Brandt, J., Christensen, J. H., Colette, A., Curci, G., Davila, Y., Dong, X., Flemming, J., Francis, X., Fraser, A., Fu, J., Henze, D. K., Hogrefe, K., Im, U., Vivanco, M. G., Jiménez-Guerrero, P., Jonson, J. E., Kitwiroon, N., Manders, A., Mathur, R., Palacios-Peña, L., Pirovano, G., Pozzoli, L., Prank, M., Schultz, M. Sokhi, R. S., Sudo, K., Tuccella, P., Takemura, T., Sekiya, T. and Unal, A. Two-scale multi-model ensemble: is a hybrid ensemble of opportunity telling us more? Atmos. Chem. Phys., 18, p. 8727-8744, 2018. DOI: 10.5194/acp-18-8727-2018

Glasius, M., Hansen, A. M. K., Claeys, M., Henzing, J. S., Jedynska, A. D., Kasper-Giebl, A., Kistler, M., Kristensen, K., Martinsson, J., Maenhaut, W., Nøjgaard, J. K., Spindler, G., Stenström, K. E., Swietlicki, E., Szidat, S., Simpson, D., Yttri, K. E. Composition and sources of carbonaceous aerosols in Northern Europe during winter. Atmospheric Environment, 173, p. 127-141, 2018. DOI: 10.1016/j.atmosenv.2017.11.005

Jonson, J. E., Schulz, M., Emmons, L., Flemming, J., Henze, D., Sudo, K., Tronstad Lund, M., Lin, M., Benedictow, A., Koffi, B., Dentener, F., Keating, T. and Kivi, R. The effects of intercontinental emission sources on European air pollution levels. Atmos. Chem. Phys., 18 (18), p. 13655-13672, 2018. DOI: 10.5194/acp-18-13655-2018

Karset, I. H. H., Berntsen, T. K., Storelvmo, T., Alterskjær, K., Grini, A., Oliviè, D. J. L., Kirkevåg, A., Seland, Ø., Iversen, T., Schulz, M. Strong impacts on aerosol indirect effects from historical oxidant changes. Atmos. Chem. Phys., 18 (10), p. 7669-7690, 2018. DOI: 10.5194/acp-18-7669-2018

Kirkevåg, A., Grini, A., Oliviè, D. J. L., Seland, Ø., Alterskjær, K., Hummel, M., Karset, I. H. H., Lewinschal, A., Liu, X., Makkonen, R., Bethke, I., Griesfeller, J., Schulz, M., Iversen, T. A production-tagged aerosol module for earth system models, OsloAero5.3-extensions and updates for CAM5.3-Oslo. Geoscientific Model Development, 11 (10) p. 3945-3982, 2018. DOI: 10.5194/gmd-11-3945-2018

Le Breton, M., Hallquist, Å., Kant Pathak, R., Simpson, D., Wang, Y., Johansson, J., Zheng, J., Yang, Y., Shang, D., Wang, H., Liu, Q., Chan, C., Wang, T., Bannan, T. J., Priestley, M., Percival, C. J., Shallcross, D. E., Lu, K., Guo, S., Hu, M., Hallquist, M. Chlorine oxidation of VOCs at a semi-rural site in Beijing: significant chlorine liberation from ClNO2 and subsequent gas- and particle-phase Cl-VOC production. Atmos. Chem. Phys., 18 (17) p. 13013-13030, 2018. DOI: 10.5194/acp-18-13013-2018

Lefohn, A. S., Malley, C. S., Smith, L., Wells, B., Hazucha, M., Simon, H., Naik, V., Mills, G., Schultz, M. G., Paoletti, E., De Marco, A., Xu, X., Zhang, L., Wang, T., Neufeld, H. S., Musselman, R. C., Tarasick, D., Brauer, M., Feng, Z., Tang, H., Kobayashi, K., Sicard, P., Solberg, S. and Gerosa, G., Tropospheric ozone assessment report: Global ozone metrics for climate change, human health, and crop/ecosystem research. Elem. Sci. Anth., 6(1), p. 28, 2018. DOI: 10.1525/elementa.279

Liang, C.-K., West, J. J., Silva, R. A., Bian, H., Chin, M., Davila, Y., Dentener, F. J., Emmons, L., Flemming, J., Folberth, G., Henze, D., Im, U., Jonson, J. E., Keating, T. J., Kucsera, T., Lenzen, A., Lin, M., Lund, M. T., Pan, X., Park, R. J., Pierce, R. B., Sekiya, T., Sudo, K., Takemura, T. HTAP2 multi-model estimates of premature human mortality due to intercontinental transport of air pollution and emission sectors. Atmos. Chem. Phys., 18, p. 10497-10520, 2018. DOI: 10.5194/acp-18-10497-2018

Lund, M. T., Myhre, G., Haslerud, A. S., Skeie, R. B., Griesfeller, J., Platt, S. M., Kumar, R., Myhre, C. L., Schulz, M. Concentrations and radiative forcing of anthropogenic aerosols from 1750 to 2014 simulated with the Oslo CTM3 and CEDS emission inventory. Geoscientific Model Development, 11, p. 4909-4931, 2018. DOI: 10.5194/gmd-11-4909-2018

Mills, G., Sharps, K., Simpson, D., Pleijel, H., Broberg, M., Uddling, J., Jaramillo, F., Davies, W. J., Dentener, F., Van den Berg, M., Agrawal, M., Agrawal, S. B., Ainsworth, E. A., Buker, P., Emberson, L., Feng, Z., Harmens, H., Hayes, F., Kobayashi, K., Paoletti, E., Van Dingenen, R. Ozone pollution will compromise efforts to increase global wheat production. Global Change Biology, 24 (8), p. 3560-3574, 2018. DOI: 10.1111/gcb.14157

Mills, G., Pleijel, H., Malley, C. S., Sinha, B., Cooper, O. R., Schultz, M. G., Neufeld, H. S., Simpson, D., Sharps, K., Feng, Z., Gerosa, G., Harmens, H., Kobayashi, K., Saxena, P., Paoletti, E., Sinha, V., Xu, X. Tropospheric ozone assessment report: Present-day tropospheric ozone distribution and trends relevant to vegetation. Elementa: Science of the Anthropocene, 6: 47, p. 1-46, 2018. DOI: 10.1525/elementa.302

Mills, G., Sharps, K., Simpson, D., Pleijel, H., Frei, M., Burkey, K., Emberson, L., Uddling, J., Broberg, M., Feng, Z., Kobayashi, K., Agrawal, M. Closing the global ozone yield gap: Quantification and cobenefits for multistress tolerance. Global Change Biology, 24 (10), p. 4869-4893, 2018. DOI: 10.1111/gcb.14381

Muri, H., Tjiputra, J., Otterå, O. H., Adakudlu, M., Lauvset, S. K., Grini, A., Schulz, M., Niemeier, U., Kristjansson, J. E. Climate response to aerosol geoengineering: a multi-method comparison. Journal of Climate, 31 (16), p. 6319-6340, 2018. DOI: 10.1175/JCLI-D-17-0620.1

Nickel, S., Schröder, W., Schmalfuss, R., Saathoff, M., Harmens, H., Mills, G., Frontasyeva, M. V., Barandovski, L., Blum, O., Carballeira, A., De Temmerman, L., Dunaev, A. M., Ene, A., Fagerli, H., Godzik, B., Ilyin, I., Jonkers, S., Jeran, Z., Lazo, P., Leblond, S., Liiv, S., Mankovska, B., Nunez-Olivera, E., Piispanen, J., Poikolainen, J., Popescu, I. V., Qarri, F., Santamaria, J. M., Schaap, M., Skudnik, M., Spiric, Z., Stafilov, T., Steinnes, E., Stihi, C., Suchara, I., Uggerud, H. T., Zechmeister, H. G. Modelling spatial patterns of correlations between concentrations of heavy metals in mosses and atmospheric deposition in 2010 across Europe. Environmental Sciences Europe, 30, 2018. DOI: 10.1186/s12302-018-0183-8

Oliver, R. J., Mercado, L. M., Sitch, S., Simpson, D., Medlyn, B. E., Lin, Y.-S., Folberth, G. A. Large but decreasing effect of ozone on the European carbon sink. Biogeosciences, 15 (13), p. 4245-4269, 2018. DOI: 10.5194/bg-15-4245-2018

Otero, N., Sillmann, J., Mar, K., Rust, H. W., Solberg, S., Andersson, C., Engardt, M., Bergström, R., Bessagnet, B., Colette, A., Couvidat, F., Cuvelier, C., Tsyro, S., Fagerli, H., Schaap, M., Manders, A., Mircea, M., Briganti, G., Cappelletti, A., Adani, M., D'Isidoro, M., Pay, M. T., Theobald, M., Vivanco, M. G., Wind, P. A., Ojha, N., Raffort, V., Butler, T. A multi-model comparison of meteorological drivers of surface ozone over Europe. Atmos. Chem. Phys., 1 (16), p. 12269-12288, 2018. DOI: 10.5194/acp-18-12269-2018

Pandolfi, M., Alados-Arboledas, L., Alastuey, A., Andrade, M., Angelov, C., Artiñano, B., Backman, J., Baltensperger, U., Bonasoni, P., Bukowiecki, N., Collaud Coen, M., Conil, S., Coz, E., Crenn, V., Dudoitis, V., Ealo, M., Eleftheriadis, K., Favez, O., Fetfatzis, P., Fiebig, M., Flentje, H., Ginot, P., Gysel, M., Henzing, B., Hoffer, A., Holubova Smejkalova, A., Kalapov, I., Kalivitis, N., Kouvarakis, G., Kristensson, A., Kulmala, M., Lihavainen, H., Lunder, C., Luoma, K., Lyamani, H., Marinoni, A., Mihalopoulos, N., Moerman, M., Nicolas, J., O'Dowd, C., Petäjä, T., Petit, J.-E., Pichon, J. M., Prokopciuk, N., Putaud, J.-P., Rodróguez, S., Sciare, J., Sellegri, K., Swietlicki, E., Titos, G., Tuch, T., Tunved, P., Ulevicius, V., Vaishya, A., Vana, M., Virkkula, A., Vratolis, S., Weingartner, E., Wiedensohler, A., and Laj, P. A European aerosol phenomenology - 6: scattering properties of atmospheric aerosol particles from 28 ACTRIS sites. Atmos. Chem. Phys., 18, p. 7877-7911, 2018. DOI: 10.5194/acp-18-7877-2018

Pommier, M., Fagerli, H., Gauss, M., Simpson, D., Sharma, S., Sinha, V., Ghude, S., Landgren, O. A., Nyiri, A., Wind, P. A. Impact of regional climate change and future emission scenarios on surface O3 and PM2.5 over India. Atmos. Chem. Phys., 18 (1), p. 103-127, 2018. DOI: 10.5194/acp-18-103-2018

Popovici, I., Goloub, P., Podvin, T., Blarel, L., Loisil, R., Mortier, A., Deroo, C., Ducos, F., Victori, S., Torres, B. A mobile system combining lidar and sunphotometer on-road measurements: Description and first results. The European Physical Journal Conferences, 176, 2018. DOI: 10.1051/epjconf/201817608003

Popovici, I., Goloub, P., Podvin, T., Blarel, L., Loisil, R., Unga, F., Mortier, A., Deroo, C., Victori, S., Ducos, F., Torres, B., Delegove, C., Choel, M., Pujol-Sohne, N., Pietras, C. Description and applications of a mobile system performing on-road aerosol remote sensing and in situ measurements. Atmospheric Measurement Techniques, 11 (8), p. 4671-4691, 2018. DOI: 10.5194/amt-11-4671-2018

Samset, B. H., Stjern, C. W., Andrews, E., Kahn, R. A., Myhre, G., Schulz, M., Schuster, G. L. Aerosol Absorption: Progress Towards Global and Regional Constraints. Current Climate Change Reports, 4 (2), p. 65-83, 2018. DOI: 10.1007/s40641-018-0091-4

Schmeisser, L., Backman, J., Ogren, J. A., Andrews, E., Asmi, E., Starkweather, S., Uttal, T., Fiebig, M., Sharma, S., Eleftheriadis, K., Vratolis, S., Bergin, M., Tunved, P., and Jefferson, A. Seasonality of aerosol optical properties in the Arctic. Atmos. Chem. Phys., 18, p. 11599-11622, 2018. DOI: 10.5194/acp-18-11599-2018

Schwede, D. B., Simpson, D., Tan, J., Fu, J. S., Dentener, F., Du, E., deVries, W. Spatial variation of modelled total, dry and wet nitrogen deposition to forests at global scale. Environmental Pollution, 243, p. 1287-1301, 2018. DOI: 10.1016/j.envpol.2018.09.084

Stadtler, S., Simpson, D., Schroder, S., Taraborrelli, D., Bott, A., Schultz, M. Ozone impacts of gas-aerosol uptake in global chemistry transport models. Atmos. Chem. Phys., 18 (5), p. 3147-3171, 2018. DOI: 10.5194/acp-18-3147-2018

Tan, J., Fu, J. S., Dentener, F., Sun, J., Emmons, L., Tilmes, S., Sudo, K., Flemming, J., Jonson, J. E., Gravel, S., Bian, H., Davila, Y., Henze, D. K., Lund, M. T., Kucsera, T., Takemura, T., Keating, T. Multi-model study of HTAP II on sulfur and nitrogen deposition. Atmos. Chem. Phys., 18 (9), p. 6847-6866, 2018. DOI: 10.5194/acp-18-6847-2018

Turnock, S. T., Wild, O., Dentener, F. J., Davila, Y., Emmons, L. K., Flemming, J., Folberth, G. A., Henze, D. K., Jonson, J. E., Keating, T, J., Kengo, S., Lin, M., Lund, M., Tilmes, S., and O'Connor, F. M. The impact of future emission policies on tropospheric ozone using a parameterised approach. Atmos. Chem. Phys., 18, p. 8953-8978, 2018. DOI: 10.5194/acp-18-8953-2018

Vivanco, M. G., Theobald, M. R., García-Gómez, H., Garrido, J. L., Prank, M., Aas, W., Adani, M., Alyuz, U., Andersson, C., Bellasio, R., Bessagnet, B., Bianconi, R., Bieser, J., Brandt, J., Briganti, G., Cappelletti, A., Curci, G., Christensen, J. H., Colette, A., Couvidat, F., Cuvelier, C., D'Isidoro, M., Flemming, J., Fraser, A., Geels, C., Hansen, K. M., Hogrefe, C., Im, U., Jorba, O., Kitwiroon, N., Manders, A., Mircea, M., Otero, N., Pay, M.-T., Pozzoli, L., Solazzo, E., Tsyro, S., Unal, A., Wind, P., and Galmarini, S. Modeled deposition of nitrogen and sulfur in Europe estimated by 14 air quality model systems: evaluation, effects of changes in emissions and implications for habitat protection. Atmos. Chem. Phys., 18, p. 10199-10218, 2018. DOI: 10.5194/acp-18-10199-2018

Wang, R., Andrews, E., Balkanski, Y., Boucher, O., Myhre, G., Samset, B. H., Schulz, M., Schuster, G. L., Valari, M., Tao, S. Spatial Representativeness Error in the Ground-Level Observation Networks for Black Carbon Radiation Absorption. Geophysical Research Letters, 45 (4), p. 2106-2114, 2018. DOI: 10.1002/2017GL076817

Werner, M., Kryzaa, M., Wind, P. A. High resolution application of the EMEP MSC-W model over Eastern Europe - Analysis of the EMEP4PL results. Atmospheric research, 212, p. 6-22, 2018. DOI: 10.1016/j.atmosres.2018.04.025

Associated EMEP reports and notes in 2019

Joint reports

Transboundary particulate matter, photo-oxidants, acidification and eutrophication components. Joint MSC-W & CCC & CEIP Report. EMEP Status Report 1/2019

EMEP MSC-W model performance for acidifying and eutrophying components, photo-oxidants and particulate matter in 2017. Supplementary material to EMEP Status Report 1/2019

CCC Technical and Data reports

Anne-Gunn Hjellbrekke. Data Report 2017. Particulate matter, carbonaceous and inorganic compounds. EMEP/CCC-Report 1/2019

Anne-Gunn Hjellbrekke and Sverre Solberg. Ozone measurements 2017. EMEP/CCC-Report 2/2019

Wenche Aas, Knut Breivik and Pernilla Bohlin Nizzetto. Heavy metals and POP measurements 2017. EMEP/CCC-Report 3/2019

Sverre Solberg, Anja Claude and Stefan Reimann. VOC measurements 2017. EMEP/CCC-Report 4/2019

CEIP Technical and Data reports

Melanie Tista and Robert Wankmüller. Methodologies applied to the CEIP GNFR gap-filling 2019. Part Ia: BC, Part Ib: Main pollutants and Particulate Matter (NO_x, NMVOCs, SO_x, NH_3, CO, $PM_{2.5}$, PM_{10}, PM_{coarse}), Technical Report CEIP 1/2019

Melanie Tista and Robert Wankmüller. Methodologies applied to the CEIP GNFR gap-filling 2019. Part II: Heavy Metals (Pb, Cd, Hg), Technical Report CEIP 2/2019

Melanie Tista and Robert Wankmüller. Methodologies applied to the CEIP GNFR gap-filling 2019. Part III: Persistent organic pollutants (Benzo(a)pyrene, Benzo(b)fluoranthene, Benzo(k)fluoranthene, Indeno(1,2,3-cd)pyrene, Total polycyclic aromatic hydrocarbons, Dioxin and Furan, Hexachlorobenzene, Polychlorinated biphenyls), Technical Report CEIP 3/2019

Marion Pinterits, Bernhard Ullrich, Silke Gaisbauer (ETC-ACM), Katarina Mareckova and Robert Wankmüller (CEIP/ETC-ACM). Inventory review 2019. Review of emission data reported under the LRTAP Convention and NEC Directive. Stage 1 and 2 review. Status of gridded and LPS data. Annexes, Joint CEIP/EEA Report. Technical Report CEIP 4/2019

Katarina Mareckova, Robert Wankmüller, Marion Pinterits and Sabine Schindlbacher. Methodology report, Technical Report CEIP 5/2019

Robert Wankmüller. Documentation of the new EMEP gridding System for the spatial disaggregation of emission data with resolution of $0.1^\circ \times 0.1^\circ$ (long-lat), Technical Report CEIP 6/2019

Sabine Schindlbacher and Robert Wankmüller. Uncertainty and recalculations of emission inventories, Technical Report CEIP 7/2019

Sabine Schindlbacher. The condensable component of particulate matter - summary of the information on the inclusion of the condensable component in PM_{10} and $PM_{2.5}$ emission factors provided by Parties, Technical Report CEIP 7/2019

MSC-W Technical and Data reports

Heiko Klein, Michael Gauss, Ágnes Nyíri and Svetlana Tsyro. Transboundary air pollution by main pollutants (S, N, O_3) and PM in 2017, Country Reports. EMEP/MSC-W Data Note 1/2019

References

Gauss, M., Hjellbrekke, A.-G., Aas, W., and Solberg, S.: Ozone, Supplementary material to EMEP Status Report 1/2019, available online at www.emep.int, The Norwegian Meteorological Institute, Oslo, Norway, 2019a.

Gauss, M., Tsyro, S., Fagerli, H., Hjellbrekke, A.-G., and Aas, W.: Acidifying and eutrophying components, Supplementary material to EMEP Status Report 1/2019, available online at www.emep.int, The Norwegian Meteorological Institute, Oslo, Norway, 2019b.

Gauss, M., Tsyro, S., Fagerli, H., Hjellbrekke, A.-G., Aas, W., and Solberg, S.: EMEP MSC-W model performance for acidifying and eutrophying components, photo-oxidants and particulate matter in 2017., Supplementary material to EMEP Status Report 1/2019, available online at www.emep.int, The Norwegian Meteorological Institute, Oslo, Norway, 2019c.

LRTAP: Mapping critical levels for vegetation, in: Manual on Methodologies and Criteria for Mapping Critical Loads and Levels and Air Pollution Effects, Risks and Trends. Revision of 2009, edited by Mills, G., UNECE Convention on Long-range Transboundary Air Pollution. International Cooperative Programme on Effects of Air Pollution on Natural Vegetation and Crops, updated version available at www.icpmapping.com/, 2009.

Mills, G. and Simpson, D.: New flux-based critical levels for ozone-efefcts on vegetation, in: Transboundary acidification, eutrophication and ground level ozone in Europe. EMEP Status Report 1/2010, pp. 123–126, The Norwegian Meteorological Institute, Oslo, Norway, 2010.

Mills, G., Hayes, F., Simpson, D., Emberson, L., Norris, D., Harmens, H., and Büker, P.: Evidence of widespread effects of ozone on crops and (semi-)natural vegetation in Europe (1990-2006) in relation to AOT40- and flux-based risk maps, Global Change Biology, 17, 592–613, doi:10.1111/j.1365-2486.2010.02217.x, 2011a.

Mills, G., Pleijel, H., Braun, S., Büker, P., Bermejo, V., Calvo, E., Danielsson, H., Emberson, L., Grünhage, L., Fernández, I. G., Harmens, H., Hayes, F., Karlsson, P.-E., and Simpson, D.: New stomatal flux-based critical levels for ozone effects on vegetation, Atmos. Environ., 45, 5064 – 5068, doi:10.1016/j.atmosenv.2011.06.009, 2011b.

Mills, G., Sharps, K., Simpson, D., Pleijel, H., Broberg, M., Uddling, J., Jaramillo, F., Davies, William, J., Dentener, F., Berg, M., Agrawal, M., Agrawal, S., Ainsworth, E. A., Büker, P., Emberson, L., Feng, Z., Harmens, H., Hayes, F., Kobayashi, K., Paoletti, E., and Dingenen, R.: Ozone pollution will compromise efforts to increase global wheat production, Global Change Biol., 24, 3560–3574, doi:10.1111/gcb.14157, URL https://onlinelibrary.wiley.com/doi/abs/10.1111/gcb.14157, 2018.

Tsyro, S., Gauss, M., Hjellbrekke, A.-G., and Aas, W.: PM10, PM2.5 and individual aerosol components, Supplementary material to EMEP Status Report 1/2019, available online at www.emep.int, The Norwegian Meteorological Institute, Oslo, Norway, 2019.

Willmott, C. J.: On the validation of models, Physical Geography, 2, 184–194, 1981.

Willmott, C. J.: Some Comments on the Evaluation of Model Performance, Bulletin American Meteorological Society, 63, 1309–1313, doi:10.1175/1520-0477(1982)063<1309:SCOTEO>2.0.CO;2, 1982.

Part I

Status of air pollution

CHAPTER 2

OLD-OLD-OLD Status of transboundary air pollution in 2017

Svetlana Tsyro, Wenche Aas, Sverre Solberg, Anna Benedictow, Hilde Fagerli and Thomas Scheuschner

This chapter describes the status of transboundary air pollution in 2017. A short summary of the meteorological conditions for 2017 is presented and the EMEP network of measurements in 2017 is briefly described. Thereafter, the status of air pollution and exceedances in 2017 is discussed.

2.1 Meteorological conditions in 2017

Air pollution is significantly influenced by both emissions and weather conditions. Temperature and precipitation are important factors and therefore a short summary describing the situation in 2017 as reported by the meteorological institutes in European and EECCA countries is given first.

The meteorological data to drive the EMEP MSC-W air quality model have been generated by the Integrated Forecast System model (IFS) of the European Centre for Medium-Range Weather Forecasts (ECMWF), hereafter referred to as the ECMWF-IFS model. In the meteorological community the ECMWF-IFS model is considered as state-of-the-art, and MSC-W has been using this model in hindcast mode to generate meteorological reanalyses for the year to be studied (Cycle 40r1 is the model version used for the year 2017 model run). Next section show temperature and precipitation in 2017 compared to the 2000-2016 average based on the same ECMWF-IFS model hindcast setup.

2.1.1 Temperature and precipitation

The mean temperature in 2017 was reported by the World Meteorological Organisation (WMO 2018) as one of the three highest on record globally, the fifth highest in Europe. According

to the Arctic Report Card 2017 (Overland et al. 2017) October 2016 to September 2017 was the second warmest on record since 1900 in the Arctic. The EMEP MSC-W model version rv4.33 has been used for the 2017 model runs. The horizontal resolution is $0.1^\circ \times 0.1^\circ$, with 20 vertical layers (the lowest with a height of approximately 50 meters).

Meteorology, emissions, boundary conditions and forest fires for 2017 have been used as input (for description of these input data see Simpson et al. 2012). The meteorological input has been derived from ECMWF-IFS(cy40r1) simulations (2.1). The land-based emissions have been derived from the 2019 official data submissions to UNECE CLRTAP (Pinterits et al. 2019), as documented in Chapter 3. Emissions from international shipping within the EMEP domain are derived from the CAMS global shipping emissions (Granier et al. 2019), developed by the Finish Meteorological Institute (FMI). The forest fires emissions are taken The Fire INventory from NCAR (FINN) (Finnigan et al. 1990), version 5. For more details on the emissions for 2017 model run see Chapter 3 and Appendix **??**.

Preliminary simulations for 2018 have been performed with the same EMEP MSC-W model version (rv4.33), driven with 2018 meteorological input (also derived from ECMWF-IFS cy40r1), and used the same emissions (anthropogenic and forest fires) as in the 2017 run. Climatological means were used for boundary conditions. No evaluation of the 2018 results have been made as EMEP observational data for 2018 were not available. The model results for 2018 can be downloaded from the EMEP webpage (`http://www.emep.int`).

Trend runs with the EMEP MSC-W model have been performed for the period of 2000–2016, using meteorological data and emissions for the respective years. The land-based emissions for 2000–2016 were derived from the 2019 official data submissions to UNECE CLRTAP (Pinterits et al. 2019), and the international shipping emissions were derived from the CAMS global shipping emission dataset (Granier et al. 2019, ECCAD 2019), produced by FMI using AIS (Automatic Identification System) tracking data (see also Appendix **??**). FINNv5 forest fire emissions have been used for corresponding years in the runs for 2002-2016, whereas for 2000 and 2001 average emissions over the 2005-2015 period have been used. Note that the SO_x emissions from the eruption of the Grimsvotn volcano in 2011 have deliberately been excluded, since the model cannot accurately simulate their dispersion as their intrusion occurred above the model's top layer.

2.2 Air pollution in 2017

2.2.1 Ozone

The ozone observed at a surface station is the net result of various physio-chemical processes; surface dry deposition and uptake in vegetation, titration by nearby NO_x emissions, regional photochemical ozone formation and atmospheric transport of baseline ozone levels, each of which may have seasonal and diurnal systematic variations. Episodes with elevated levels of ozone are observed during the summer half year when certain meteorological situations (dry, sunny, cyclonic stable weather) promotes the formation of ozone over the European continent.

Figure **??** shows various modelled ozone metrics for 2017 with the corresponding measured metrics based on the EMEP measurement sites plotted on top of the maps. Figure **??** show similar plots with data from Airbase measurement sites. Note that most of the EMEP sites are also classified as Airbase sites and thus included in Figure **??** as well. Only stations located below 500 metres above sea level were used in this comparison to avoid uncertain-

ties related to the extraction of model data in regions with complex topography. The maps show a) the mean of the daily max concentration for the 6-months period April-September, b) SOMO35 (= Sum of Ozone Means Over 35 ppb), c) AOT40 for forests (= Accumulated Ozone exposure over a Threshold of 40 ppb) for the 6-months period April-September using the hours between 08 and 20 and d) POD_1 for forests (= Phytotoxic Ozone Dose above a threshold 1 mmol m^{-2}) (only for Figure **??**). POD_1 could not be calculated from the ozone monitoring data directly and are thus not given in plot d).

The mean daily max O_3, SOMO35 and AOT40 all show a distinct gradient with levels increasing from north to south, a well established feature for ozone in general reflecting the dependency of ozone on the photochemical conditions. Ozone formation is promoted by solar radiation and high temperatures. The highest levels of these ozone metrics are predicted over the Mediterranean Ocean and in the southeast corner of the model grid. The measurement network are limited to the continental western part of the model domain with no valid data in Belarus, Ukraine, Turkey or the area further east.

For the region covered by the monitoring sites, the pattern with increased levels to the south with maximum levels near the Mediterranean is seen in the measurement data as well as the model. The geographical pattern in the measured values are fairly well reflected by the model results for all these three metrics. In particular, the modelled mean daily max for the summer half year agrees very well with the measured values. Particularly high levels are predicted by the model in the southeast, but due to the lack of monitoring sites these levels could not be validated.

A good agreement between modelled and observed levels of SOMO35 and AOT40 is also seen from Figure **??** and Figure **??**. It should be noted that the O_3 metrics such as AOT40 are very sensitive to the calculation of vertical O_3 gradients between the middle of the surface layer and the 3m height used for comparison with measurements (Tuovinen et al. 2007) and thus more difficult to compare with measurement data than e.g. the mean daily maximum. Indeed, the formulation we use (Simpson et al. 2012) is probably better suited to a first model layer of 90m height (since we equate the centre of this, ca. 45m, with a 'blending-height') than to a first level of 50m height (as used throughout this report).

The modelled POD_1 pattern differs from the other metrics reflecting the influence of additional parameters such as plant physiology, soil moisture etc., and is a metric more indicative of the direct impact of ozone on vegetation than e.g. AOT40. The POD_1 field could however not be validated by the EMEP ozone measurement data alone.

SOMO35 is an indicator for health impact assessment recommended by WHO, and the results given in Figure **??** and Figure **??** indicates that the health risk associated with surface ozone increased towards southern Europe in 2017. SOMO35 is a health risk indicator without any specific threshold or limit value.

AOT40 and POD_1 are indicators for effects on vegetation. UN-ECE's critical level for forests is 5000 ppb hours, and the measurements given in Figure **??** and Figure **??** indicate that this level was exceeded in most of the European continent in 2017 whereas it was not exceeded in most of Scandinavia and the British Isles. As mentioned, the model predicts larger areas with exceedances than the measurements. For POD_1 the limit value depends on the species and Mills et al (2011) give a value of 4 mmol m^{-2} for birch and beech and 8 mmol m^{-2} for Norway spruce. The results in Figure **??** indicate that both these limit values were exceeded in most of Europe. The modelled levels of POD_1 could, however, not be validated by observations.

A more detailed comparison between model and measurements for ozone for the year 2017 can be found in Gauss et al. (2019).

Ozone episodes in 2017

The surface ozone levels are closely connected to the weather conditions and in particular to the temperature. As shown in Figure **??** a) the 2m summer temperatures were lower than normal in Germany, Poland and Scandinavia in 2017 and slightly above the normal in the UK and France. As discussed above, a stronger positive temperature anomaly was seen in the Mediterranean, in particular in Spain and Portugal.

This is reflected in the occurrence of ozone episodes. Relatively few marked episodes was experienced in central and northern Europe whereas in the south, the Po Valley and the Iberian peninsula experienced a number of episodes of smaller regional extent. In the following, three episodes affecting larger parts of the European continent are presented briefly - one in the end of May, one in the last part of June and the last one in the beginning of August.

28 - 29 May

This episode was linked to a high pressure located over central Europe and low pressures west of Spain/France setting up a southerly flow of warm air into central Europe. The episode lasted only a couple of days and affected mainly the Netherlands, Germany and northern Italy. The episode peaked on 29 May when several sites crossed EU's information threshold of 180

μg m^{-3} and two sites experienced ozone levels above 200 μg m^{-3} . On 30 May the warm air mass had moved to the east with lower ozone levels. As shown in Figure **??** and Figure **??** the model captures the area of elevated ozone very well but apparently underpredicts the daily maximum ozone in some areas, particularly Belgium and the Netherlands.

References

ECCAD: Emissions of atmospheric Compounds and Compilation of Ancillary Data, URL https://eccad.aeris-data.fr, 2019.

Finnigan, J. J., Raupach, M. R., Bradley, E. F., and Aldis, G. K.: A Wind-Tunnel Study Of Turbulent-Flow Over A 2-Dimensional Ridge, Boundary-Layer Meteorology, 50, 277–317, 1990.

Gauss, M., Tsyro, S., Fagerli, H., Hjellbrekke, A.-G., Aas, W., and Solberg, S.: EMEP MSC-W model performance for acidifying and eutrophying components, photo-oxidants and particulate matter in 2017., Supplementary material to EMEP Status Report 1/2019, available online at www.emep.int, The Norwegian Meteorological Institute, Oslo, Norway, 2019.

Granier, C., Darras, S., Denier van der Gon, H., Doubalova, J., Elguindi, N., Galle, B., Gauss, M., Guevara, M., Jalkanen, J.-P., Kuenen, J., Liousse, C., Quack, B., Simpson, D., and Sindelarova, K.: The Copernicus Atmosphere Monitoring Service global and regional emissions (April 2019 version), doi:10.24380/d0bn-kx16, URL https://atmosphere.copernicus.eu/sites/default/files/2019-06/cams_emissions_general_document_apr2019_v7.pdf, 2019.

Overland, J., Hanna, E., Hanssen-Bauer, I., Kim, S.-J., Walsh, J., Walsh, J. E., Wang, M., Bhatt, U. S., and Thoman, R. L.: Surface Air Temperature, in Arctic Report Card 2017, NOAA, http://www.arctic.noaa.gov/Report-Card/Report-Card-Archive, 2017.

Pinterits, M., Ullrich, B., Gaisbauer, S., Mareckova, K., and Wankmüller, R.: Inventory review 2019. Review of emission data reported under the LRTAP Convention and NEC Directive. Stage 1 and 2 review. Status of gridded and LPS data, EMEP/CEIP 4/2019, CEIP/EEA Vienna, 2019.

Simpson, D., Benedictow, A., Berge, H., Bergström, R., Emberson, L. D., Fagerli, H., Hayman, G. D., Gauss, M., Jonson, J. E., Jenkin, M. E., Nyíri, A., Richter, C., Semeena, V. S., Tsyro, S., Tuovinen, J.-P., Valdebenito, A., and Wind, P.: The EMEP MSC-W chemical transport model – technical description, Atmos. Chem. Physics, 12, 7825–7865, doi:10.5194/acp-12-7825-2012, 2012.

Tuovinen, J.-P., Simpson, D., Ashmore, M., Emberson, L., and Gerosa, G.: Robustness of modelled ozone exposures and doses, Environ. Poll., 146, 578–586, 2007.

WMO: WMO Statement on the State of the Global Climate in 2017, WMO-No. 1212, https://public.wmo.int/en/resources/library, ISBN 978-92-63-11212-5, 2018.

CHAPTER 3

OLD-OLD-OLD Emissions for 2017

Silke Gaisbauer, Robert Wankmüller, Bradley Matthews, Katarina Mareckova, Sabine Schindlbacher, Carlos Sosa, Melanie Tista and Bernhard Ullrich

In addition to meteorological variability, changes in the emissions affect the inter-annual variability and trends of air pollution, deposition and transboundary transport. The main changes in emissions in 2017 with respect to previous years are documented in the following sections.

The EMEP Reporting guidelines (UNECE 2014) requests all Parties to the LRTAP Convention to report annually emissions and activity data of air pollutants (SO_x[1], NO_2[2], NMVOCs[3], NH_3, CO, HMs, POPs, PM[4] and voluntary BC). Further, every four years, projection data, gridded data and information on large point sources (LPS) have to be reported to the EMEP Centre on Emission Inventories and Projections (CEIP).

3.1 Reporting of emission inventories in 2019

Completeness and consistency of submitted data have improved significantly since EMEP started collecting information on emissions. Data of at least 45 Parties each year were submit-

[1]"Sulphur oxides (SO_x)" means all sulphur compounds, expressed as sulphur dioxide (SO_2), including sulphur trioxide (SO_3), sulphuric acid (H_2SO_4), and reduced sulphur compounds, such as hydrogen sulphide (H_2S), mercaptans and dimethyl sulphides, etc.

[2]"Nitrogen oxides (NO_x)" means nitric oxide and nitrogen dioxide, expressed as nitrogen dioxide (NO_2).

[3]"Non-methane volatile organic compounds" (NMVOCs) means all organic compounds of an anthropogenic nature, other than methane, that are capable of producing photochemical oxidants by reaction with nitrogen oxides in the presence of sunlight.

[4]"Particulate matter" (PM) is an air pollutant consisting of a mixture of particles suspended in the air. These particles differ in their physical properties (such as size and shape) and chemical composition. Particulate matter refers to:
(i) "$PM_{2.5}$", or particles with an aerodynamic diameter equal to or less than 2.5 micrometers (μm);
(ii) "PM_{10}", or particles with an aerodynamic diameter equal to or less than 10 (μm).

ted to CEIP for the last seven years (see Figure **??**). 45 Parties (88%) submitted inventories[5] in 2019; six Parties[6] did not submit any data and 39 Parties reported black carbon (BC) emissions (see section 3.2). Although 2019 was no reporting year for large point sources (LPS), gridded emissions and projections, three Parties reported information on LPS, five Parties reported gridded data in new resolution, and twenty-five Parties reported projection data (Pinterits et al. 2019).

The quality of the submitted data across countries differs quite significantly. By compiling the inventories, countries have to use the newest available version of the EMEP/EEA air pollutant emission inventory guidebook, which is the version of 2016 (EMEP/EEA 2016). However, many countries still use the 2013 Guidebook (EMEP/EEA 2013) or older versions. Uncertainty of the reported data (national totals, sectoral data) is considered relatively high, the completeness of reported data has not turned out satisfactory for all pollutants and sectors either.

Detailed information on recalculations, completeness and key categories, plus additional review findings can be found in the annual EEA & CEIP technical inventory review reports (Pinterits et al. 2019) and its Annexes[7].

3.2 Black Carbon (BC) emissions

Over the last decade, black carbon (BC) has emerged as one of the most important anthropogenic air pollutants. Due to its distinct physical properties and its potential toxicity (Janssen et al. (2012)) BC is a significant air pollutant in terms of both climate change and air quality. Given its absorption spectrum in the visible range, BC warms the atmosphere directly by absorbing solar radiation and, indirectly, by accelerating snow-/ice melt when deposited (Bond et al. (2013)). According to recent estimates, the direct radiative forcing effect of black carbon emissions during the first part of the industrial era may have been of the same magnitude as methane (CH_4) emissions (Bond et al. (2013), Wang et al. (2016)). Meanwhile, in terms of human health, epidemiological studies suggest that certain pulmonary and cardiovascular conditions are more strongly associated with exposure to BC rather than aggregate PM (e.g. Baumgartner et al. (2014)). The emerging significance of BC is mirrored in developments in the international policy arena. Since the Executive Body Decision 2013/04, Parties to the LRTAP Convention have been formally encouraged to submit inventory estimates of their national BC emissions, and in 2015 the reporting templates were updated to include BC data emissions. In addition to reporting under CLRTAP, EU member states are also encouraged to submit BC emissions estimates as part of their emissions reporting under the National Emissions Ceilings (NEC) Directive (2016/2284/EU). Furthermore, in the context of the particularly acute impacts of BC in accelerating climate change in the Arctic (Sand et al. (2016)), ministers of the Arctic Council adopted the *Enhanced Black Carbon and Methane Emissions Reductions: An Arctic Council Framework Action* which committed the Arctic States (Canada, Denmark, Finland, Iceland, Norway, Russia, Sweden and United States of America) to develop and submit emissions inventories for BC and CH_4 to the Council.

Under the auspices of the *EU Action on Black Carbon in the Arctic* (EUA-BCA) a tech-

[5]The original submissions from the Parties can be accessed via the CEIP homepage on `http://www.ceip.at/status_reporting/2019_submissions`.

[6]Greece, Bosnia and Herzegovina, Kazakhstan, Liechtenstein, the Republic of Moldova, and Montenegro

[7]`http://www.ceip.at/review_proces_intro/review_reports`

nical report, *Review of Reporting Systems for National Black Carbon Emissions Inventories*, was recently compiled. The report, which was co-led by CEIP and will soon be published on the Action's website[8], reviewed, *inter alia*, the level of BC reporting under the LRTAP Convention. Despite a large number of Parties voluntarily reporting BC emissions, the review revealed a number of shortcomings. As of 2018, nine Parties had not yet submitted BC emissions inventories to the Convention. Furthermore, analysis of the emissions estimates which were reported revealed significant issues in terms of consistency, completeness and comparability. As an example, Figure **??** illustrates the varying level of reporting of BC emissions for the sector *Residential combustion* N14 1A4bi. The review thus highlights that caution should be taken when utilizing and/or analyzing BC emissions reported by the CLRTAP Parties.

Beyond this report CEIP continues to monitor and review the level of BC reporting by the Convention's Parties. Below a brief overview of BC emissions estimates submitted by EMEP countries in 2019 is given.

Twenty-one countries (out of 39) submitted a complete time series of national total BC emissions (1990-2017), 31 submitted a complete time series from 2000 onwards. Figure **??** shows the 2000-2017 BC emissions trends for those 31 Parties. Most Parties (24) report a negative trend, with the emissions of 22 Parties decreasing by 20% or more. Six Parties report an increase in emissions when comparing the 2017 and 2000 estimates.

Figure **??** gives an overview on the BC emissions reported for the year 2017. Thirty-eight of 39 reporting Parties reported emissions for 2017. The United States reported BC emissions data in 2019, however, the most recent estimate is for the year 2014. As the upper part of the graph illustrates, for the majority of these Parties, 2017 BC emissions constitute between 10 and 20% of the respective total $PM_{2.5}$ emissions. Indeed the median BC fraction based on reported BC and $PM_{2.5}$ emissions lies at 15.01%.

For more detailed information on BC consult the annual EEA & CEIP technical inventory review report (Pinterits et al. 2019).

3.3 Inclusion of the condensable component in PM emissions

The condensable component of particulate matter is probably the biggest single source of uncertainty in PM emissions. Currently the condensable component is not included or excluded consistently in PM emissions reported by Parties of the LRTAP Convention. Also in the EMEP/EEA Guidebook (EMEP/EEA 2016) the condensable fraction is not consistently included or excluded in the emission factors, but improvements are planned for the 2019 update of the EMEP/EEA Guidebook. However, PM emissions reported by Parties to the LRTAP Convention are not directly comparable at the moment with implications on the modeling of overall exposure to PM compliance with $PM_{2.5}$ emissions reduction commitments.

Parties were asked to include a table with information on the inclusion of the condensable component in PM_{10} and $PM_{2.5}$ emission factors for the reporting under the CLRTAP convention in 2019. This table has been added to the revised recommended structure for IIRs[9]. Seventeen Parties provided information on the inclusion of the condensable component in PM_{10}

[8] https://eua-bca.amap.no/

[9] https://www.ceip.at/ms/ceip_home1/ceip_home/reporting_instructions/annexes_to_guidelines/

and $PM_{2.5}$ emission factors (Austria, Belgium, Croatia, Estonia, Germany, Finland, France, Latvia, the Netherlands, Portugal, Romania, Slovakia, Slovenia, Spain, Sweden, Switzerland and United Kingdom)[10]. Eleven of these Parties provided the information in the recommended format. Some Parties chose to report the information on an aggregated level. This reporting is a first step towards a better understanding of the reported PM data. However, the reporting in 2019 showed that in many cases Parties do not have the information if the PM emissions of a specific source category include the condensable component. For the majority of the source categories of PM emission Parties either indicated that it is "unknown" if the condensable component is included in the PM emissions, or they provided no information or the provided information was not clear. The status of inclusion or exclusion is best known for the emissions from road transport. For example for "1A3bi Road transport passenger cars" ten of the twelve Parties that provided information for this source category report emissions to be included and only two Parties state that the status of inclusion is unknown.

Small-scale combustion sources make a notable contribution to total PM emissions. For all Parties that reported $PM_{2.5}$ emissions for "1A4bi Residential: Stationary" for the year 2017[11] emissions from this source category contributed 44% to the national total $PM_{2.5}$ emissions. Small-scale combustion is one of the sources where the inclusion of the condensable component has the largest impact on the emission factor. For example, for conventional woodstoves, one of the most important categories in Europe, the emission factors excluding and including the condensable fractions may differ by up to a factor of five (Denier van der Gon et al. 2015). Here the status of the inclusion was less clear. Of the thirteen Parties that provided information for "1A4bi Residential: Stationary" three parties reported the condensable component to be included and three Parties to be excluded. The other Parties reported "unknown", "partially included" or provided information on a more detailed level with different status of inclusion (see Table **??**).

As 2019 was the first year in which Parties were asked to provide information on the inclusion of the condensable component, it is expected that the reporting will improve over the coming years, with more parties reporting the information and with a higher quality of the reported information.

3.4 Comparison of 2016 data (reported in 2018) and 2017 data (reported in 2019)

The comparison of 2016 emissions (reported in 2018) and 2017 emissions (reported in 2019) showed, that for 21 countries data changed by more than 10% for one or several pollutants (see Figure **??** and Table **??**-**??**). These changes can be caused by real emission reductions or increases, or recalculations made by the respective country.

In five countries, both NO_x and CO emissions changed by more than 10%. For NMVOCs, emissions changed in two countries by more than 10%. For SO_x, emissions changed by more than 10% in 14 countries, while for NH_3 the change of emission levels were less than 10% in each country. Of the PMs, emissions changed by more than 10% in ten countries for $PM_{2.5}$, in seven countries for PM_{10} and in nine countries for PM_{coarse}[12] (see Figure **??** and Table **??**-**??**).

[10] Status 30 April 2019

[11] Status 2 May 2019

[12] PM_{coarse} emissions are not reported by Parties but calculated as difference between PM_{10} and $PM_{2.5}$ emissions.

The largest changes occurred in Belarus, Kyrgyzstan, Malta and Ukraine.

References

Baumgartner, J., Zhang, Y., Schauer, J. J., Huang, W., Wang, Y., and Ezzati, M.: Highway proximity and black carbon from cookstoves as a risk factor for higher blood pressure in rural China, PNAS 111, 36, 13 229–13 234, doi:doi:10.1073/pnas.1317176111, 2014.

Bond, T. C., Doherty, S. J., Fahey, D. W., Forster, P. M., Berntsen, T., DeAngelo, B. J., Flanner, M. G., Ghan, S., Kärcher, B., Koch, D., Kinne, S., Kondo, Y., Quinn, P. K., Sarofim, M. C., Schultz, M. G., Schulz, M., Venkataraman, C., Zhang, H., Zhang, S., Bellouin, N., Guttikunda, S. K., Hopke, P. K., Jacobson, M. Z., Kaiser, J. W., Klimont, Z., Lohmann, U., Schwarz, J. P., Shindell, D., Storelvmo, T., Warren, S. G., and Zender, C. S.: Bounding the role of black carbon in the climate system: A scientific assessment, J. Geophys. Res., 118, 5380–5552, doi:10.1002/jgrd.50171, 2013.

Denier van der Gon, H. A. C., Bergström, R., Fountoukis, C., Johansson, C., Pandis, S. N., Simpson, D., and Visschedijk, A. J. H.: Particulate emissions from residential wood combustion in Europe - revised estimates and an evaluation, Atmos. Chem. Physics, pp. 6503–6519, doi:doi:10.5194/acp-15-6503-2015, URL http://www.atmos-chem-phys.net/15/6503/2015/, 2015.

EMEP/EEA: EMEP/EEA air pollutant emission inventory guidebook - 2013, 12/2013, European Environment Agency, EEA, URL http://www.eea.europa.eu/publications/emep-eea-guidebook-2013, 2013.

EMEP/EEA: EMEP/EEA air pollutant emission inventory guidebook - 2016, 21/2016, European Environment Agency, EEA, URL http://www.eea.europa.eu/publications/emep-eea-guidebook-2016, 2016.

Janssen, N. A. H., Gerlofs-Nijla, M. E., Lanki, T., Salonen, R. O., Cassee, F., Hoek, G., Fischer, P., Brunekreef, B., and Krzyzanowsi, M.: Health effects of black carbon, World Health Organization, pp. 1–96, URL http://www.euro.who.int/__data/assets/pdf_file/0004/162535/e96541.pdf, 2012.

Pinterits, M., Ullrich, B., Gaisbauer, S., Mareckova, K., and Wankmüller, R.: Inventory review 2019. Review of emission data reported under the LRTAP Convention and NEC Directive. Stage 1 and 2 review. Status of gridded and LPS data, EMEP/CEIP 4/2019, CEIP/EEA Vienna, 2019.

Sand, M., Berntsen, T. K., von Salzen, K., Flanner, M. G., Langner, J., and Victor, D. G.: Response of Arctic temperature to changes in emissions of short-lived climate forcers, Nat. Clim. Change, 6, 286–290, doi:10.1038/nclimate2880, 2016.

UNECE: Guidelines for reporting emission data under the Convention on Long-range Transboundary Air Pollution, Tech. Rep. ECE/EB.AIR/130, UNECE, URL http://www.ceip.at/fileadmin/inhalte/emep/2014_Guidelines/ece.eb.air.125_ADVANCE_VERSION_reporting_guidelines_2013.pdf, 2014.

Wang, R., Balkanski, Y., Boucher, O., Ciais, P., Schuster, G. L., Chevallier, F., Samset, B. H., Liu, J., Piao, S., Valari, M., and Tao, S.: Estimation of global black carbon direct radiative

forcing and its uncertainty constrained by observations., J. Geophys. Res. Atmos., 121, 5948–5971, doi:10.1002/2015JD024326, URL https://agupubs.onlinelibrary.wiley.com/doi/epdf/10.1002/2015JD024326, 2016.

Part II

Research Activities

Part III

Technical EMEP Developments

CHAPTER 4

OLD-OLD-OLD Updates to the EMEP MSC-W model, 2018-2019

David Simpson, Robert Bergström, Svetlana Tsyro and Peter Wind

This chapter summarises the changes made to the EMEP MSC-W model since Simpson et al. (2018), and along with changes discussed in Simpson et al. (2013), Tsyro et al. (2014), Simpson et al. (2015, 2016, 2017), updates the standard description given in Simpson et al. (2012). The model version used for reporting this year is denoted rv4.33, which has some significant changes since the rv4.17a documented last year. Table 4.3 summarises the changes made in the EMEP model since the version documented in Simpson et al. (2012).

4.1 Overview of changes

- EmChem19 – a new gas-phase chemical mechanism has been introduced (Bergström et al., 2019), updating the EmChem16x scheme used previously. See Sect. 4.2.
- CRI v2.2a-emep – the Common Reactive Intermediates (CRI) mechanism (Jenkin et al. 2008) used in research versions of the EMEP model has been updated and a new isoprene scheme for the CRI scheme has been implemented in the model (Jenkin et al. 2019, McFiggans et al. 2019).
- The carbon-bond scheme used in research versions of the EMEP model has been updated from CB05 (Yarwood et al. 2005) to CB6r2 (Luecken et al. 2019).
- Two new schemes for handling secondary organic aerosol (SOA) have been added to the model – a new volatility basis set (VBS) scheme from Hodzic et al. (2016), that takes into account recent findings regarding high formation rates for SOA, and an alternative "1.5-dimensional" volatility basis set (VBS) scheme, based on Koo et al. (2014), which handles both oxygenation and fragmentation of primary and secondary OA by atmospheric oxidation (chemical aging), in a simplified way.

- The EMEP 3D model and chemical pre-processing systems (GenChem) were re-harmonised, making use of a new python-based system. See Sect. 4.3.
- We have added 'EQSAM4clim' as an option for aerosol thermodynamics. See Sect. 4.4.
- A bug-fix for radiation (PAR) was also needed, with significant impact on POD calculations for forests. See Sect. 4.5.
- New methods to specify emissions inputs were added, which allow more flexible input of data from external sources. See Sect. 4.6.
- The vertical profiles of emission releases were modified, reflecting the transition to a finer resolution of the modelling grid and as a part of the general model development towards a flexible code
- The use of configuration files was again expanded, replacing some of the earlier hard-coded methods to specify model setups. See Sect. 4.8.

4.2 EmChem19 chemical mechanism

The new gas-phase chemistry scheme – EmChem19 – is a substantial revision of the EmChem16 scheme (Simpson et al. 2017). The reaction rates in EmChem19 are updated to be consistent with the latest recommendations from the IUPAC (IUPAC 2019, Atkinson et al. 2004, 2006), and evaluated against the latest Master Chemical Mechanism (MCM v3.3.1, Jenkin et al. 2015, and refs therein). In addition to these updates (and bug fixes) some new gas-phase reactions have been added and a few new chemical species have been included in the chemical mechanism. Major changes compared to EmChem16 include:

- The addition of benzene and toluene as emitted species.
- A revised (very simplified) aromatic chemistry – tuned to give reasonably good agreement with the Master Chemical Mechanism (MCM, see Jenkin et al. 2015) in box model simulations.
- Addition of more than 20 new reactions – including a number of reactions between peroxy and nitrate radicals and a new treatment of peroxy - peroxy radical reactions, using the total RO_2 pool as a reactant.
- Changes of the rates and/or products of ca 45 reactions.
- Revised SOA formation from sesquiterpenes (SQT) – in EmChem19 SQT emissions are assumed to be equal to 5% (by mass) of the monoterpene emissions; in the model the emitted SQT is assumed to immediately form non-volatile BSOA, with 17% yield (mass based).
- A few reactions were removed or simplified compared to EmChem16 – this includes a simplification of the minimal scheme for monoterpene chemistry (based on Lamarque et al. 2012), which was introduced in EmChem16; in the standard EmChem19 scheme monoterpenes are modelled using a single surrogate MT (APINENE) instead of the three used in EmChem16.

A detailed description of the EmChem19 scheme, including evaluation against ambient measurements and comparison to the MCM and other chemical mechanisms in box model simulations, will be given by Bergström et al., 2019.

4.3 Revised GenChem system

.

The chemical mechanism files used in the EMEP CTM have for many years been generated with a chemical pre-processor. Originally written in perl, GenChem.pl, and now in python, GenChem.py, this pre-processor reads files which describe the chemical mechanism using chemical notation (e.g. krate OH + NO2 = HNO3), and produces differential equations in fortran, ready for import into the EMEP source code as the CM_ files (e.g. CM_ChemSpecs_mod.f90). GenChem.pl used to be a part of the emepctm package as used at MSC-W, but now GenChem.py is part of a separate system which allows testing of chemical mechanisms with either a box-model (BoxChem) or the 1-D Ecosystem Surface Exchange model (ESX, Simpson and Tuovinen 2014). With this system the EMEP model chemistry can be evaluated against more advanced and well-evaluated schemes such as the Master Chemical Mechanism (MCM, e.g. Jenkin et al. 2015, Saunders et al. 2003, CRI (Jenkin et al. 2019) or carbon-bond (Yarwood et al. 2005, Luecken et al. 2019).

4.4 EQSAM4clim

Three thermodynamic equilibrium models are currently implemented in the EMEP MSC-W model to calculate gas/aerosol partitioning of inorganic semi-volatile species. The alternative models are: Ammonium (EMEP simplified equilibrium scheme, Hov et al. 1988), MARS (Binkowski and Shankar 1995), and EQSAM (Metzger and Lelieveld 2007). The MARS scheme, presently used in the standard model, has some limitations, the major one being the number of chemical species included in the thermodynamic equlibrium, but also the assumption of metastable aqueous aerosols. This year, a new version of EQSAM - EQSAM4clim (Metzger et al. 2016) - has been implemented as an optional thermodynamic scheme. The advantage of the scheme is that it considers a full gas-liquid-solid partitioning and can account for more cations (e.g. Na^{+}, Ca^{2+}, Mg^{2+}) and anions (Cl^{-}). Preliminary testing of EQSAM4clim has been carried out, and the results are presented in Chapter **??**. Further evaluation of the scheme with more observations, as well as its testing in source-receptor calculations are needed before the EQSAM4clim can be considered for use in EMEP MSC-W reporting runs.

4.5 Radiation issues

As noted in Simpson et al. (2018), the radiation scheme of Weiss and Norman (1985) was introduced in order to give better estimates of diffuse versus direct photosynthetically active radiation (PAR), and to fix a bug in the calculations of these variables which had been identified in previous model versions. PAR is used in modelling both stomatal uptake and biogenic VOC emissions. Unfortunately this bug-fix contained itself a bug in the units used in the stomatal uptake (DO3SE) module, so that calculated PAR levels were too low. This has now

Figure 4.1: Comparison of model versions rv4.33 and rv4.32 for mean ozone (top-left), POD1 for IAM deciduous forests (top-right) and POD_3IAM for crops (bottom). The dashed line represents the 1:1 line. Calculations are for the year 2012, using the 50km version of the model.

been corrected. As found and explained in Simpson et al. (2018), and illustrated in Fig. 4.1, the impact of the change is mainly apparent for forests. The net result of fixing this bug is to restore POD levels to very similar levels to those seen in the rv4.15 version discussed in Simpson et al. (2018). As before, the correlation coefficient between new and old versions is very high ($\geq$0.996).

4.6 Emission inputs

A new system for reading emissions has been implemented. The new system allows to read emissions in NetCDF, without the need of heavy preprocessing of these inputs. Any 2-dimensional emission field can be directly used by the model, provided the longitude and latitude data is provided. The metadata, such as species, units, names, sectors, etc. can be provided separately in the configuration file, if they are not found in the emission file. The new system is at present implemented in addition to the previous one, and emissions in both formats can be used at the same time.

An emission mask can be defined using any field in a NetCDF file. This mask can then be used to reduce emission over the region covered by the mask.

4.7 Emission heights

As documented in EMEP Status Report 1/2016 (2016), the release heights of GNFR sectoral emissions are assigned based on those previously developed for the SNAP system. The heights of emission release are now expressed in pressure levels, as documented in Table 4.1. Here, the P-levels indicate air pressure at the top of the layer, within which the given fraction of emissions is released. The lowest layer (second column) is confined between 101325.0 Pa (the surface) and 101084.9 Pa (appr. 20m), etc. The vertical profiles of emission releases have been slightly modified, using the experiences of EMEP (Simpson et al. 2012) and EuroDelta (Bessagnet et al. 2014).

These emission vertical profiles are defined independently of the model's actual vertical layers. Thus, the emissions layers do not necesserily match model layers, and the emissions are then redistributed into actual model layers. For the model levels used in the runs for this report, the final emission release vertical profiles are shown in Table 4.2. Note that compared to earlier runs, the thickness of the lowest layer is now decreased from 92 m to about 50 m.

4.8 Configuration

The configuration parameters of the model run is entirely steered through a fortran namelist. The file can easily be edited, to provide alternative parameters and paths to the input data. Some key changes are:

Table 4.1: Definition used for the fractions of emissions, released within a given vertical layer, defined by pressure (P) levels. The P-levels are pressure (Pa) at the top of corresponding layer (P Surface = 101325.0 Pa). The approximate heights (ΔZ, m) of the layer boundaries are also included.

P-level	101084.9	100229.1	99133.2	97489.35	95206.225	92283.825	88722.15
ΔZ (m)	0 - 20	20 - 92	92 - 184	184 - 324	324 - 522	522-781	781-1106
GNFR 1	0.0	0.00	0.0025	0.1475	0.40	0.30	0.15
GNFR 2	0.06	0.16	0.75	0.03	0.00	0.00	0.0
GNFR 3	1.0	0.00	0.00	0.00	0.00	0.00	0.0
GNFR 4	0.05	0.15	0.70	0.10	0.00	0.00	0.0
GNFR 5	1.0	0.00	0.00	0.00	0.00	0.00	0.0
GNFR 6	1.0	0.00	0.00	0.00	0.00	0.00	0.0
GNFR 7	1.0	0.00	0.00	0.00	0.00	0.00	0.0
GNFR 8	1.0	0.00	0.00	0.00	0.00	0.00	0.0
GNFR 9	1.0	0.00	0.00	0.00	0.00	0.00	0.0
GNFR 10	0.0	0.00	0.41	0.57	0.02	0.00	0.0
GNFR 11	1.0	0.00	0.00	0.00	0.00	0.00	0.0
GNFR 12	1.0	0.00	0.00	0.00	0.00	0.00	0.0
GNFR 13	0.02	0.08	0.60	0.30	0.00	0.00	0.0

- Many small changes to make model configuration easier and more flexible; see the User Guide for further explanation of some new methods and possibilities.

- The ‘femis’ file used to control emission changes per country and sector was developed further, and can now use country codes (e.g. ‘SE’) rather than numbers (e.g. 18) to specify the source to be modified.

- The configuration file is now organized in one large namelist instead of several ones. This will reduce the chances for syntactic errors.

Table 4.2: The fractions of emissions, released within the actual model layers, for which the approximate heights (ΔZ, m) of their boundaries are also shown.

ΔZ (m)	0 - 50	50 - 94	94 - 155	155 - 237	237 - 341	341 - 623	623 - 1015	1015 -1522
GNFR 1	0.000	0.000	0.002	0.056	0.125	0.485	0.290	0.042
GNFR 2	0.127	0.111	0.498	0.245	0.019	0.000	0.000	0.000
GNFR 3	1.000	0.000	0.000	0.000	0.000	0.000	0.000	0.000
GNFR 4	0.113	0.104	0.465	0.256	0.062	0.000	0.000	0.000
GNFR 5	1.000	0.000	0.000	0.000	0.000	0.000	0.000	0.000
GNFR 6	1.000	0.000	0.000	0.000	0.000	0.000	0.000	0.000
GNFR 7	1.000	0.000	0.000	0.000	0.000	0.000	0.000	0.000
GNFR 8	1.000	0.000	0.000	0.000	0.000	0.000	0.000	0.000
GNFR 9	1.000	0.000	0.000	0.000	0.000	0.000	0.000	0.000
GNFR 10	0.000	0.010	0.272	0.342	0.357	0.018	0.000	0.000
GNFR 11	1.000	0.000	0.000	0.000	0.000	0.000	0.000	0.000
GNFR 12	1.000	0.000	0.000	0.000	0.000	0.000	0.000	0.000
GNFR 13	0.054	0.061	0.398	0.300	0.187	0.000	0.000	0.000

4.9 Nesting

A full snapshot of the model concentrations can be saved at specific given dates, in addition to the standard modes for periodically saving boundary conditions. Typically those can be used to be used as initial conditions for a new run in a finer grid.

4.10 Biomass burning emissions

It is easy now to switch between different schemes for forest fires emissions by simply specifying the source in the configuration file (FINN, GFAS or GFED). No need to recompile the code. The vertical distribution of those emission takes into account the layer thickness.

4.11 WRF

When WRF meteorological input is used, the model height of the surface is read from the parameter 'HGT', instead of an ad hoc separate file (topography.nc).

The model will now treat correctly the singularity at the Poles in the 'lon lat' projection.

4.12 Outputs

The time stamp of the NetCDF output is now defined in the middle of the period, instead of the end.

Table 4.3: Summary of major EMEP MSC-W model versions from 2012–2017. Extends Table S1 of Simpson et al. 2012

Version	Update	Ref[(a)]
rv4.33	Public domain (June 2019) EmChem19, PAR bug-fix, EQSAM4clim	This report
rv4.32	Used for EMEP course, April 2019	
rv4.30	Moved to new GenChem-based system	
rv4.17a	Used for R2018. Small updates	R2018
rv4.17	Public domain (Feb. 2018)	R2018
	Corrections in global land-cover/deserts; added 'LOTOS' option for European NH_3 emissions; corrections to snow cover	R2018
rv4.16	New radiation scheme (Weiss&Norman); Added dry and wet deposition for N_2O_5; (Used for Stadtler et al. 2018, Mills et al. 2018b)	R2018
rv4.15	EmChem16 scheme	R2017
rv4.14	Updated chemical scheme	R2017
rv4.12	New global land-cover and BVOC	R2017
rv4.10	Public domain (Oct. 2016) (Used for Mills et al. 2018a)	R2016
rv4.9	Updates for GNFR sectors, DMS, sea-salt, dust, S_A and γ, N_2O_5	
rv4.8	Public domain (Oct. 2015) ShipNOx introduced. Used for EMEP HTAP2 model calculations, see see acp special issue: `https://www.atmos-chem-phys.net/special_issue390.html`). Also for Jonson et al. (2017).	R2015
rv4.7	Used for reporting, summer 2015 : New calculations of aerosol surface area; ; New gas-aerosol uptake and N_2O_5 hydrolysis rates ; Added 3-D calculations pf aerosol extinction and AODs; ; Emissions - new flexible mechanisms for interpolation and merging sources ; Global - monthly emissions from ECLIPSE project ; Global - LAI changes from LPJ-GUESS model ; WRF meteorology (Skamarock and Klemp 2008) can now be used directly in EMEP model.	R2015
rv4.6	Used for Euro-Delta SOA runs Revised boundary condition treatments ; ISORROPIA capability added	R2015
rv4.5	Sixth open-source (Sep 2014) Improved dust, sea-salt, SOA modelling ; AOD and extinction coefficient calculations updated ; Data assimilation system added ; Hybrid vertical coordinates replace earlier sigma ; Flexibility of grid projection increased.	R2014
rv4.4	Fifth open-source (Sep 2013) ; Improved dust and sea-salt modelling ; AOD and extinction coefficient calculations added ; gfortran compatibility improved	R2014, R2013
rv4.3	Fourth public domain (Mar. 2013) ; Initial use of namelists ; Smoothing of MARS results ; Emergency module for volcanic ash and other events; Dust and road-dust options added as defaults ; Advection algorithm changed	R2013
rv4.0	Third public domain (Sep. 2012) As documented in Simpson et al. (2012)	R2013

Notes: (a) R2018 refers to EMEP Status report 1/2018, etc.

References

Atkinson, R., Baulch, D. L., Cox, R. A., Crowley, J. N., Hampson, R. F., Hynes, R. G., Jenkin, M. E., Rossi, M. J., and Troe, J.: Evaluated kinetic and photochemical data for atmospheric chemistry: Volume I - gas phase reactions of O_x, HO_x, NO_x and SO_x species, Atmos. Chem. Physics, 4, 1461–1738, URL http://www.atmos-chem-phys.net/4/1461/2004/, 2004.

Atkinson, R., Baulch, D. L., Cox, R. A., Crowley, J. N., Hampson, R. F., Hynes, R. G., Jenkin, M. E., Rossi, M. J., Troe, J., and Subcommittee, I.: Evaluated kinetic and photochemical data for atmospheric chemistry: Volume II – gas phase reactions of organic species, Atmos. Chem. Physics, 6, 3625–4055, URL http://www.atmos-chem-phys.net/6/3625/2006/, 2006.

Bergström, R. et al.: Updating the chemical schemes of the EMEP MSC-W model; EmChem19, CRI v2.2a-emep, CB6r2-emep, In preperation, pp. –, 2019.

Bessagnet, B., Colette, A., Meleux, F., Rouïl, L., Ung, A., Favez, O., Cuvelier, C., Thunis, P., Tsyro, S., Stern, R., Manders, A., Kranenburg, R., Aulinger, A., Bieser, J., Mircea, M., Briganti, G., Cappelletti, A., Calori, G., Finardi, S., Silibello, C., Ciarelli, G., Aksoyoglu, S., Prévot, A., Pay, M.-T., Baldasano, J. M., Vivanco, M. G., Garrido, J. L., Palomino, I., Martín, F., Pirovano, G., Roberts, P., Gonzalez, L., White, L., Menut, L., Dupont, J.-C., Carnevale, C., and Pederzoli, A.: The EURODELTA III exercise – Model evaluation with observations issued from the 2009 EMEP intensive period and standard measurements in Feb/Mar 2009. TFMM & MSC-W 1/2014, Tech. rep., ., 2014.

Binkowski, F. and Shankar, U.: The Regional Particulate Matter Model .1. Model description and preliminary results, J. Geophys. Res., 100, 26 191–26 209, 1995.

EMEP Status Report 1/2016: Transboundary particulate matter, photo-oxidants, acidifying and eutrophying components, EMEP MSC-W & CCC & CEIP, Norwegian Meteorological Institute (EMEP/MSC-W), Oslo, Norway, 2016.

Hodzic, A., Kasibhatla, P. S., Jo, D. S., Cappa, C. D., Jimenez, J. L., Madronich, S., and Park, R. J.: Rethinking the global secondary organic aerosol (SOA) budget: stronger production, faster removal, shorter lifetime, Atmos. Chem. Physics, 16, 7917–7941, doi:10.5194/acp-16-7917-2016, URL http://www.atmos-chem-phys.net/16/7917/2016/, 2016.

Hov, Ø., Eliassen, A., and Simpson, D.: Calculation of the distribution of NO_x compounds in Europe., in: Troposheric ozone. Regional and global scale interactions, edited by Isaksen, I., pp. 239–262, D. Reidel, Dordrecht, 1988.

IUPAC: IUPAC Task Group on Atmospheric Chemical Kinetic Data Evaluation, URL http://iupac.pole-ether.fr, accessed: 2019-06-13, 2019.

Jenkin, M., Khan, M., Shallcross, D., Bergström, R., Simpson, D., Murphy, K., and Rickard, A.: The CRI v2.2 reduced degradation scheme for isoprene, Atmos. Environ., 212, 172 – 182, doi:https://doi.org/10.1016/j.atmosenv.2019.05.055, URL http://www.sciencedirect.com/science/article/pii/S1352231019303607, 2019.

Jenkin, M. E., Watson, L. A., Utembe, S. R., and Shallcross, D. E.: A Common Representative Intermediates (CRI) mechanism for VOC degradation. Part 1: Gas phase mechanism development, Atmos. Environ., 42, 7185–7195, doi:10.1016/j.atmosenv.2008.07.028, 2008.

Jenkin, M. E., Young, J. C., and Rickard, A. R.: The MCM v3.3.1 degradation scheme for isoprene, Atmos. Chem. Physics, 15, 11 433–11 459, doi:10.5194/acp-15-11433-2015, 2015.

Jonson, J. E., Borken-Kleefeld, J., Simpson, D., Nyíri, A., Posch, M., and Heyes, C.: Impact of excess NOx emissions from diesel cars on air quality, public health and eutrophication in Europe, Environ. Res. Lett., 12, 094 017, URL http://stacks.iop.org/1748-9326/12/i=9/a=094017, 2017.

Koo, B., Knipping, E., and Yarwood, G.: 1.5-Dimensional volatility basis set approach for modeling organic aerosol in {CAMx} and {CMAQ}, Atmospheric Environment, 95, 158 – 164, doi:http://dx.doi.org/10.1016/j.atmosenv.2014.06.031, 2014.

Lamarque, J. F., Emmons, L. K., Hess, P. G., Kinnison, D. E., Tilmes, S., Vitt, F., Heald, C. L., Holland, E. A., Lauritzen, P. H., Neu, J., Orlando, J. J., Rasch, P. J., and Tyndall, G. K.: CAM-chem: description and evaluation of interactive atmospheric chemistry in the Community Earth System Model, Geoscientific Model Dev., 5, 369–411, doi:10.5194/gmd-5-369-2012, 2012.

Luecken, D., Yarwood, G., and Hutzell, W.: Multipollutant modeling of ozone, reactive nitrogen and HAPs across the continental US with CMAQ-CB6, Atmos. Environ., 201, 62 – 72, doi:https://doi.org/10.1016/j.atmosenv.2018.11.060, URL http://www.sciencedirect.com/science/article/pii/S1352231018308434, 2019.

McFiggans, G., Mentel, T. F., Wildt, J., Pullinen, I., Kang, S., Kleist, E., Schmitt, S., Springer, M., Tillmann, R., Wu, C., Zhao, D., Hallquist, M., Faxon, C., Le Breton, M., Hallquist, A. M., Simpson, D., Bergström, R., Jenkin, M. E., Ehn, M., Thornton, J. A., Alfarra, M. R., Bannan, T. J., Percival, C. J., Priestley, M., Topping, D., and Kiendler-Scharr, A.: Secondary organic aerosol reduced by mixture of atmospheric vapours, Nature, 565, 587–593, 2019.

Metzger, S. and Lelieveld, J.: Reformulating atmospheric aerosol thermodynamics and hygroscopic growth into fog, haze and clouds, Atmos. Chem. Physics, 7, 3163–3193, 2007.

Metzger, S., Steil, B., Abdelkader, M., Klingmüller, K., Xu, L., Penner, J. E., Fountoukis, C., Nenes, A., and Lelieveld, J.: Aerosol water parameterisation: a single parameter framework, Atmospheric Chemistry and Physics, 16, 7213–7237, doi:10.5194/acp-16-7213-2016, URL https://www.atmos-chem-phys.net/16/7213/2016/, 2016.

Mills, G., Sharps, K., Simpson, D., Pleijel, H., Broberg, M., Uddling, J., Jaramillo, F., Davies, William, J., Dentener, F., Berg, M., Agrawal, M., Agrawal, S., Ainsworth, E. A., Büker, P., Emberson, L., Feng, Z., Harmens, H., Hayes, F., Kobayashi, K., Paoletti, E., and Dingenen, R.: Ozone pollution will compromise efforts to increase global wheat production, Global Change Biol., 24, 3560–3574, doi:10.1111/gcb.14157, URL https://onlinelibrary.wiley.com/doi/abs/10.1111/gcb.14157, 2018a.

Mills, G., Sharps, K., Simpson, D., Pleijel, H., Frei, M., Burkey, K., Emberson, L., Uddling, J., Broberg, M., Feng, Z., Kobayashi, K., and Agrawal, M.: Closing the global ozone yield gap: Quantification and cobenefits for multistress tolerance, Global Change Biology, 0, doi:10.1111/gcb.14381, URL https://onlinelibrary.wiley.com/doi/abs/10.1111/gcb.14381, 2018b.

Saunders, S. M., Jenkin, M. E., Derwent, R. G., and Pilling, M. J.: Protocol for the development of the Master Chemical Mechanism, MCM v3 (Part A): tropospheric degradation of non-aromatic volatile organic compounds, Atmos. Chem. Physics, 3, 161–180, URL http://www.atmos-chem-phys.net/3/161/2003/, 2003.

Simpson, D. and Tuovinen, J.-P.: ECLAIRE Ecosystem Surface Exchange model (ESX), in: Transboundary particulate matter, photo-oxidants, acidifying and eutrophying components. Status Report 1/2014, pp. 147–154, The Norwegian Meteorological Institute, Oslo, Norway, 2014.

Simpson, D., Benedictow, A., Berge, H., Bergström, R., Emberson, L. D., Fagerli, H., Hayman, G. D., Gauss, M., Jonson, J. E., Jenkin, M. E., Nyíri, A., Richter, C., Semeena, V. S., Tsyro, S., Tuovinen, J.-P., Valdebenito, A., and Wind, P.: The EMEP MSC-W chemical transport model – technical description, Atmos. Chem. Physics, 12, 7825–7865, doi:10.5194/acp-12-7825-2012, 2012.

Simpson, D., Tsyro, S., Wind, P., and Steensen, B. M.: EMEP model development, in: Transboundary acidification, eutrophication and ground level ozone in Europe in 2011. EMEP Status Report 1/2013, The Norwegian Meteorological Institute, Oslo, Norway, 2013.

Simpson, D., Tsyro, S., and Wind, P.: Updates to the EMEP/MSC-W model, in: Transboundary particulate matter, photo-oxidants, acidifying and eutrophying components. EMEP Status Report 1/2015, pp. 129–138, The Norwegian Meteorological Institute, Oslo, Norway, 2015.

Simpson, D., Nyíri, A., Tsyro, S., Valdebenito, Á., and Wind, P.: Updates to the EMEP/MSC-W model, in: Transboundary particulate matter, photo-oxidants, acidifying and eutrophying components. EMEP Status Report 1/2016, The Norwegian Meteorological Institute, Oslo, Norway, 2016.

Simpson, D., Bergström, R., Imhof, H., and Wind, P.: Updates to the EMEP MSC-W model, 2016-2017, in: Transboundary particulate matter, photo-oxidants, acidifying and eutrophying components. EMEP Status Report 1/2017, The Norwegian Meteorological Institute, Oslo, Norway, 2017.

Simpson, D., Bergström, R., , Gauss, M., Tsyro, S., Wind, P., and Valdebenito, Á.: Updates to the EMEP MSC-W model, 2017-2018, in: Transboundary particulate matter, photo-oxidants, acidifying and eutrophying components. EMEP Status Report 1/2018, The Norwegian Meteorological Institute, Oslo, Norway, 2018.

Skamarock, W. C. and Klemp, J. B.: A time-split nonhydrostatic atmospheric model for weather research and forecasting applications, J. Comp. Phys., 227, 3465–3485, doi:10.1016/j.jcp.2007.01.037, 2008.

Stadtler, S., Simpson, D., Schröder, S., Taraborrelli, D., Bott, A., and Schultz, M.: Ozone impacts of gas–aerosol uptake in global chemistry-transport models, Atmos. Chem. Physics, 18, 3147–3171, doi:10.5194/acp-18-3147-2018, URL https://www.atmos-chem-phys.net/18/3147/2018/, 2018.

Tsyro, S., Karl, M., Simpson, D., Valdebenito, A., and Wind, P.: Updates to the EMEP/MSC-W model, in: Transboundary particulate matter, photo-oxidants, acidifying and eutrophying components. EMEP Status Report 1/2014, pp. 143–146, The Norwegian Meteorological Institute, Oslo, Norway, 2014.

Weiss, A. and Norman, J. M.: Partitioning Solar-radiation into Direct and Diffuse, Visible and Near-infrared Components, Agricultural and Forest Meteorology, 34, 205–213, doi:10.1016/0168-1923(85)90020-6, 1985.

Yarwood, G., Rao, S., Yocke, M., and Whitten, G.: Updates to the Carbon Bond chemical mechanism: CB05, Final report to the US EPA, RT-0400675, December 8, 2005, Yocke and Company, URL www.camx.com/publ/pdfs/CB05_Final_Report_120805.pdfS, 2005.

CHAPTER 5

OLD-OLD-OLD Developments in the monitoring network, data quality and database infrastructure

Wenche Aas, Anne Hjellbrekke and Kjetil Tørseth

5.1 Compliance with the EMEP monitoring strategy

The monitoring obligations in EMEP are defined by the Monitoring Strategy for 2010-2019 (UNECE (2009), Tørseth et al. (2012)). The complexity in the monitoring program with respect to the number of variables and sites, whether parameters are a level 1 or level 2, and the required time resolution (hourly, daily, weekly), makes it challenging to assess whether a country is in compliance. CCC has developed an index to illustrate to what extent the Parties comply, how implementation compares with other countries, and how activities evolve with time.

For the level 1 parameters an index is defined, calculated based on what has been reported compared to what is expected. EMEP recommends one site pr 50.000 km^2, but this target number is adjusted for very large countries (i.e. KZ, RU, TR and UA). The components and number of variables to be measured in accordance to the strategy are as follows: major inorganic ions in precipitation (10 variables), major inorganic components in air (13 variables), ozone (1 variable), PM mass (2 variables) and heavy metals in precipitation (7 variables). For heavy metals, the sampling frequency is weekly, and for the other components it is daily or hourly (ozone). Based on the relative implementation of the different variables, the index has been given the following relative weights: Inorganics in precipitation: 30%, inorganics in air: 30%, ozone: 20%, PM mass: 10%, heavy metals: 10%.

Figure 5.1 summarises implementation in 2017 compared to 2000, 2005 and 2010. The countries are sorted from left to right with increasing index for 2017. Slovenia has a full score as they measure all the required parameters with satisfactory sampling frequency. Estonia, The Netherlands, Slovakia, Denmark, and Switzerland have almost complete program with an

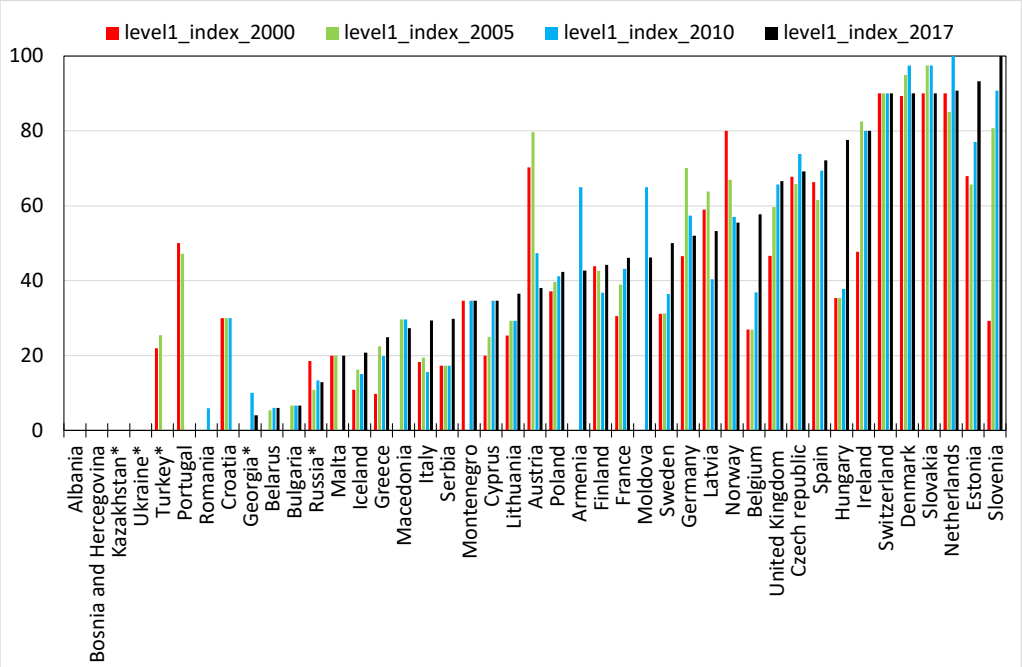

Figure 5.1: Index for implementation of the EMEP monitoring strategy, level 1 based on what has been reported for 2000, 2005, 2010 and 2016. * means adjusted land area.

index of 90% or higher. Small countries with requirements of less number of level 1 sites seem to comply easier than large countries. Since 2010, 40% of the Parties have improved their monitoring programme, while 33% have a decrease. Improvements are seen in e.g. Germany and Latvia. One Party, Malta, has reported data in 2017 and not in 2010, while Croatia and Romania have stopped reporting/measuring. In Figure **??** in Chapter **??**, the geographical distribution of level 1 sites is shown for 2017. In large parts of Europe, implementation of the EMEP monitoring strategy is far from satisfactory.

For the level 2 parameters, an index based system has not been defined, but mapping the site distribution illustrate the compliance to the monitoring strategy. 45 sites from 18 different Parties reported at least one of the required EMEP level 2 parameters relevant to this report (aerosols (36 sites), photo-oxidants (19 sites) and trace gases (9 sites)). The sites with measurements of POPs and heavy metals are covered in the EMEP status report published by MSC-E. Figure **??** shows that level 2 measurements of aerosols have better spatial coverage than oxidant precursors (VOC + methane) and trace gases. Few sites have a complete measurement program, and only 8 sites have a complete aerosol program. Nevertheless, regarding the aerosol monitoring, there have been large improvements in the spatial coverage and the data quality over the last decade. Standardization and reference methodologies have been developed, and the reporting has improved significantly with much more metadata information available. For oxidant precursors and trace gases, there are ongoing improvement in the measurement capabilities resulting from development in ACTRIS (Aerosols, Clouds, and Trace gases Research InfraStructure Network) and in co-operation with the WMO Global

Atmospheric Watch Programme (GAW).

References

Tørseth, K., Aas, W., Breivik, K., Fjæraa, A. M., Fiebig, M., Hjellbrekke, A. G., Lund Myhre, C., Solberg, S., and Yttri, K. E.: Introduction to the European Monitoring and Evaluation Programme (EMEP) and observed atmospheric composition change during 1972–2009, Atmos. Chem. Physics, 12, 5447–5481, doi:10.5194/acp-12-5447-2012, URL http://www.atmos-chem-phys.net/12/5447/2012/, 2012.

UNECE: Progress in activities in 2009 and future work. Measurements and modelling (acidification, eutrophication, photooxidants, heavy metals, particulate matter and persistent organic pollutants). Draft revised monitoring strategy., Tech. Rep. ECE/EB.AIR/GE.1/2009/15, UNECE, URL http://www.unece.org/env/documents/2009/EB/ge1/ece.eb.air.ge.1.2009.15.e.pdf, 2009.

Part IV

Appendices